Dissertation

On

THERMAL PERFORMANCE OF LOW FLUX SOLAR COLLECTOR USING CuO – H_2O BASED NANOFLUID

Submitted in partial fulfillment of the requirements for the award of degree of

Master of Engineering

IN

Thermal Engineering

Submitted by

PRASHANT SHARMA

Roll No: 801083022

Under the guidance of

Mr. Kundan Lal

Assistant Professor

Mechanical Engineering Department

Thapar University, Patiala

MECHANICAL ENGINEERING DEPARTMENT
THAPAR UNIVERSITY

PATIALA – 147004

DECLARATION

I, "**Prashant Sharma**", hereby certify that the work which is being presented in this thesis entitled "**Themal Performance of Low Flux Solar Collector using CuO – H_2O based Nanofluid**" by me in partial fulfillment of the requirements for the award of degree of Master of Engineering in Thermal Engineering from Thapar University, Patiala, is an authentic record of my own work carried out under the supervision of "Mr. Kundan lal, Assistant Professor, MED".

The matter embodied in this thesis has not been submitted in any other University / Institute for the award of any other degree.

Prashant Sharma 6/7/12

Date: 6/7/12

(PRASHANT SHARMA)

Reg. No. 801083022

This is to certify that the above statement made by the student concerned is correct to the best of my knowledge and belief.

Date: 6/7/12

6/7/12

(Mr. KUNDAN LAL)
Assistant Professor
Mechanical Engineering Department
Thapar University, Patiala

Countersigned by:

(Dr. AJAY BATISH)
Professor and Head
Mechanical Engineering Department
Thapar University,
Patiala - 147004

(Dr. S.K. MOHAPATRA)
Dean of Academic Affairs
Thapar University
Patiala – 147004

ACKNOWLEDGEMENT

I express my sincere gratitude to **Mr. Kundan Lal**, *Assistant Professor***,** Mechanical Engineering Department Thapar University, Patiala for his valuable guidance, constructive suggestions and constant encouragement in the nurturing work.

I also pay my thanks to **Dr. S.S.Mallick,** *Assistant Prof.* MED for their valuable directions and advices. I am grateful to **Dr. Ajay Batish**, *Prof. & Head*, MED for providing the facilities for the completion of the work.

I also express my thanks to the faculty and staff of **Mechanical Engineering Department Thapar University, Patiala,** for their help, inspiration and moral support. Above all, I express my indebtedness to the "*ALMIGHTY*" for his blessings and kindness.

PRASHANT SHARMA

Reg. No. 801083022

ABSTRACT

In this developing world, energy demand is growing day by day. But due to the scarcity and continuous depletion of conventional fuels, Renewable energy is an alternative source. Among all renewable energies, we have solar energy in abundance and solar collectors are commonly used to harvest the energy.

The conventional fluids which are used as the heat transfer medium in solar collectors, suffer from poor thermal and heat absorption properties. It has been found that these conventional fluids have a limited capacity to carry heat up, which in turn limits the collector performance. It has been observed that for conventional fluids, suspending the nanoparticles in a liquid (Nanofluid) can be a good substitute because of the improved thermal properties. A new type solar collector named 'Direct Solar Absorption System' (DASC) is used as the experimental set-up. DASC is more efficient collector then the conventional type solar collector, as in DASC the fluid absorbs solar thermal energy volumetrically and thus captures more heat energy. Being a new technology, a very few research has been done in the past years and it has seen that Solar collector efficiency enhanced by 4 – 5 % than the conventional fluids. Reported experimental work pertains to the application of nanofluids and performance check of the solar collectors and it is found that by using $CuO - H_2O$ nanofluid, collector performance increases up to 6 %, for mass flow rate of 60 to 100ml/hr. The collector efficiency is also affected by the volume fraction of nanoparticles. In thesis work it is reported that at higher volume concentration the problem of settle down of nanoparticles increases, which results in lowering the collector efficiency. As volume fraction goes down from 0.05% to 0.005%, efficiency is increased by a value of 2% – 2.5% on an average. This collector efficiency enhancement can be achieved up to 10 – 15 %, by overcome the problem e.g. settling down of nanoparticles, make this suitable for higher mass flow rate.

INDEX

LIST OF FIGURES

Performance Comparison Charts:-

(ii) Water vs CuO nanofluid (volume fraction – 0.005%)

(iii)CuO nanofluid (volume fraction – 0.05%) vs (Volume fraction – 0.005%)

LIST OF TABLES

ABBREVIATIONS

Symbols

K	Thermal Conductivity
Φ	% of Volume Fraction
n	Shape factor
m	mass flow rate
η	Collector Efficiency
C	Specific Heat
T	Temperature
G_T	Solar Irradiation
A	Solar Collector Area
V	Volume
v	Volume flow rate
W	Weight
ρ	Density
Ra_1	Volumetric Solar Absorption Resistance
Rcv	Convection Resistance
Rcd	Conduction Resistance
Ra_2, Rb_3	Fluid to fluid heat transfer Resistance
Rb_1	Absorption Resistance
C_r	Correction Factor
Qa	Heat absorbed by the solar collector
Qi	Total Av. Solar Radiation fall on the collector

Subscripts

eff	Nanofluid
f	Base Fluid
P	Nanoparticle

1 Initial Condition

2 Final Condition

CHAPTER 1

INTRODUCTION

1.1 Solar Energy

Sun is the main source of energy in solar system. It offers us the energy of great potential in terms of supplying the world's need. As the primary energy resources are depleting continuously, solar energy draws attention of researchers throughout the world. Solar energy is one of the alternative energies that have vast potential. It is estimated that the earth receives approximately 1000W/m^2 amount of solar irradiation in a day [15].The solar radiation incident on the Earth's surface is comprised of two types of radiation – beam and diffuse, ranging in the wavelengths from the ultraviolet to the infrared (300 to 200 nm), which is characterized by an average solar surface temperature of approximately 6000°K [16]. The amount of this solar energy that is intercepted is 5000 times greater than the sum of all other inputs – terrestrial nuclear, geothermal and gravitational energies, and lunar gravitational energy [17]. To put this into perspective, if the energy produced by 25 acres of the surface of the sun were harvested, there would be enough energy to supply the current energy demand of the world.

When solar radiation incident on a surface then some of this radiation is absorbed and in turn, increase the temperature of the surface. As the temperature of the body increases, the surface loses heat at an increasing rate to the surroundings. Steady-state is reached when the rate of the solar heat gain is balanced by the rate of heat loss to the ambient surroundings [19].

The total energy received from the sun, per unit time, on a surface of unit area kept perpendicular to the radiation, in space, just outside the earth's atmosphere is known as Solar Constant. The value of the solar constant is about 1350 w/m^2 [20].

Extraterrestrial solar radiation is the solar radiation which falls on a surface normal to the rays of the sun outside the atmosphere of the earth. This extraterrestrial solar radiation at the mean earth-sun distance is called the solar constant. As the extraterrestrial solar radiation passes through the atmosphere, part of it is reflected

back into space, part is absorbed by air and water vapor, and some is scattered. The solar radiation that reaches the surface of the earth is known as beam (direct) radiation, and the scattered radiation that reaches the surface from the sky is known as sky diffuse radiation.

1.2 Solar Energy Collector

The conversion of Solar Thermal Energy into more usable form (e.g. Heat or Electricity) is done by solar energy collectors. A solar collector is a device which transfers the collected solar energy to a fluid passing in contact with it, so it is always a matter of investigation to know that how efficiently solar collectors are converting solar energy into thermal energy [11].

The Classification of solar collectors is:

(i) Non-Concentrating or flat plate type solar collector

(ii) Concentrating type solar collector

Non-Concentrating solar collector:

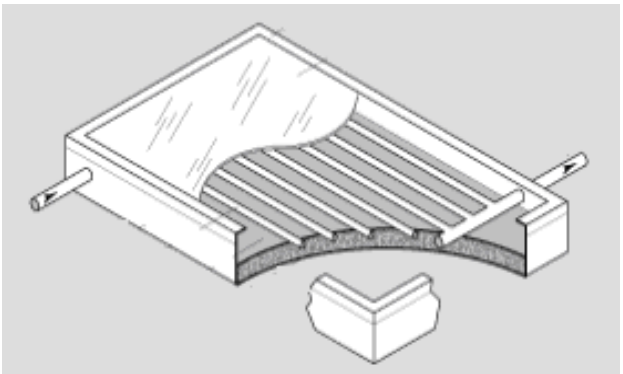

Fig.1.1 (Cross-sectional view of Flat plate collector) [8]

Concentrating Type solar collector:

(Parabolic trough)

(Dish type collector)

Fig 1.2 (Concentrating solar collector)

The most commonly used of the solar collectors are the flat plate collectors. Flat plate collectors, developed by HOTTEL and WHILLIER in the 1950s. Flat plate collector is an insulated box with the glazing (glass or plastic cover) and a dark colored absorber plate. These collectors heat up liquid or air at temperature less then 80˚C. Flat plate collectors are further classified based on fluid used (e.g. Liquid heating collector or solar air hater). The main components are:

Fig. 1.3 [9]

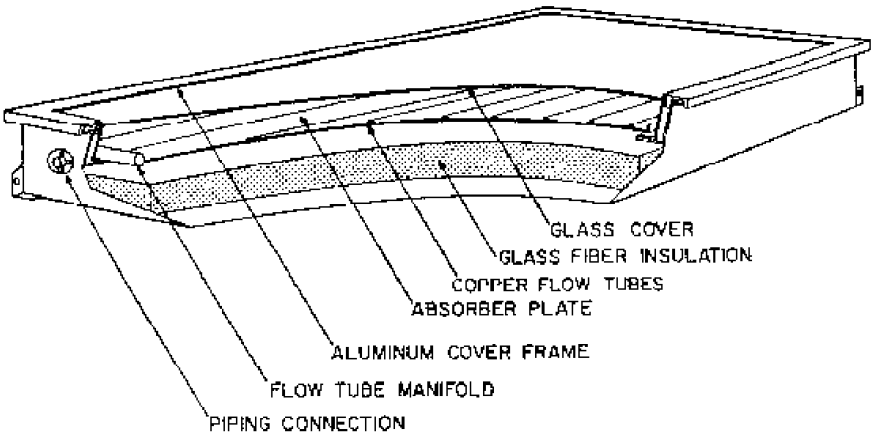

1.2.1 Direct Absorption Solar Collector

To enhance the efficiency of the solar collectors the system is made to directly absorb the solar energy with in the fluid volume and thus so called Direct Absorption Solar Collector (DASC) [1]. The schematic diagram is shown in Fig 1.3. This diagram shows the comparison between DASC and conventional flat plate collector. In Conventional flat plate collector fluid absorbs heat energy through surface absorber (fluid flow through pipes) where as in DASC solar heat is directly absorbed by the fluid. So, in turn DASC cuts down the heat resistance then conventional flat plate collector. The equation given below shows that the

total resistance of conventional flat plate collector is much higher then DASC system.

$Ra_1 + Ra_2 < Rb_1 + Rb_2 + Rb_3$

Where, $Rb_2 = Rcv + Rcd$

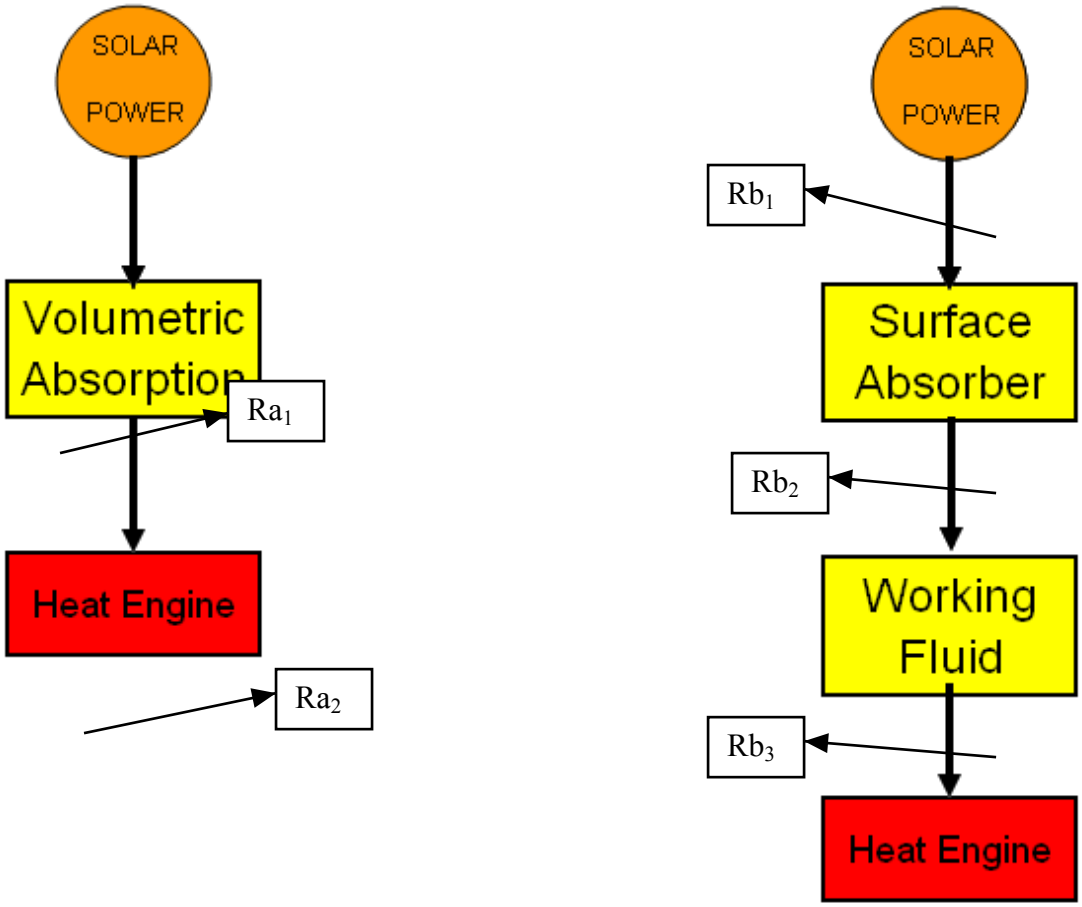

(a) (b)

Fig 1.4 (a. DASC, b. Conventional flat plate collector)

The performance of collector not only depends on how effective the absorber is but also how effective is the heat transfer and thermal properties (e.g. Thermal Conductivity, Heat capacity) of the fluid. The absorption properties of the fluids generally used in solar collectors are very poor which in turn limits the efficiency of the solar collector.

So, there is a need to use energy – efficient heat transfer fluids for high efficiency. This need can be fulfilled by using Nanofluids in solar collectors.

1.2.2 Factors effecting performance of solar collector

There are various factors, which affect the performance of solar collector [13].

Some of them are as follows

1. Absorber Surface Material
2. No. of Glazing covers
3. Spacing between the Cover and Plate as well as with the second cover
4. Effect of Shading
5. Collector Tilt
6. Thermal properties of working Fluid used in collectors.

1.3 Nanofluids

The term Nanofluids is coined by Choi (1995). The suspension of nano - particles into the fluids are known as Nanofluids [2]. Nanomaterials have unique mechanical, Optical, Electrical, Magnetic and Thermal properties with an average sizes below 100nm. A very small amount of nanoparticles when dispersed in any host fluids (e.g. Water, Oil, Ethlyene Glycol) can improve the thermal properties of fluids dramatically.

The materials used for making nanoparticles are as follows:

1. Oxide ceramics (Al_2O_3, CuO)
2. Nitride Ceramics (AlN, SiN)
3. Carbide Ceramics (SiC, TiC)
4. Metals (Cu, Ag, Au)
5. Semiconductors (TiO_2, SiC)
6. Carbon Nanotubes

7. Composite Materials ($Al_{70}Cu_{30}$)

Nanoparticles can be manufactured by mainly two processes, those are Physical Processes and Chemical Processes. Physical Processes include Inert Gas Condensation (IGC) and mechanical grinding and Chemical Processes include Chemical vapor deposition (CVD), Chemical precipitation, micro emulsion, Thermal spray and Spray pyrolysis.

For making Nanofluids, nanoparticles are suspended in conventional heat transfer fluids in two ways:

1. Two Step Method
2. Single Step Method

In Two Step method first nanoparticles are fabricated and then disperse nanoparticles into the base fluids where as in Single Step method making and dispersion of nanoparticle happens simultaneously. Two step methods are most widely used for preparing Nanofluids. One step methods can not be used to synthesis nanofluids on a large scale and the cost of production is also very high. One step methods are complex in operation.

One of the methods to enhance the performance of the solar heating systems is to introduce the nanofluid in solar water heater instead of conventional heat transfer systems (like water). Conventional fluids have a poor heat transfer properties, which is the primary obstacle to the high compactness and effectiveness of the system. The essential initiative is to seek the solid particles suspension in the base fluid with improved thermal properties than those of conventional fluids [5]. Also nanofluids show higher density then conventional fluids, which increase the heat absorbing capacity of nanofluids. So, in renewable energy industry, nanofluids can be employed to enhance heat transfer from solar collectors to storage tanks and to increase the energy density.

CHAPTER 2

LITERATURE REVIEW

In the literature review, here is the discussion of all the literatures that have been studied. The literature consist research papers mainly from the solar collectors and application of nanofluids in solar energy.

The literatures based on solar energy collectors are reviewed and the variations of efficiency to some parameters e.g. solar radiation, mass flow rate, temperature difference etc are studied.

Literature of Nanofluids application in solar collectors is studied profoundly. The detailed review on literature is as follows:

Otanicar P T *et al.* [3]

This paper is a report on the practical results of nanofluids based solar collectors, in the experiment nanofluids are manufactured using varity of nanoparticles (Carbon Nanotubes, graphite and silver). The experimental set-up is shown below.

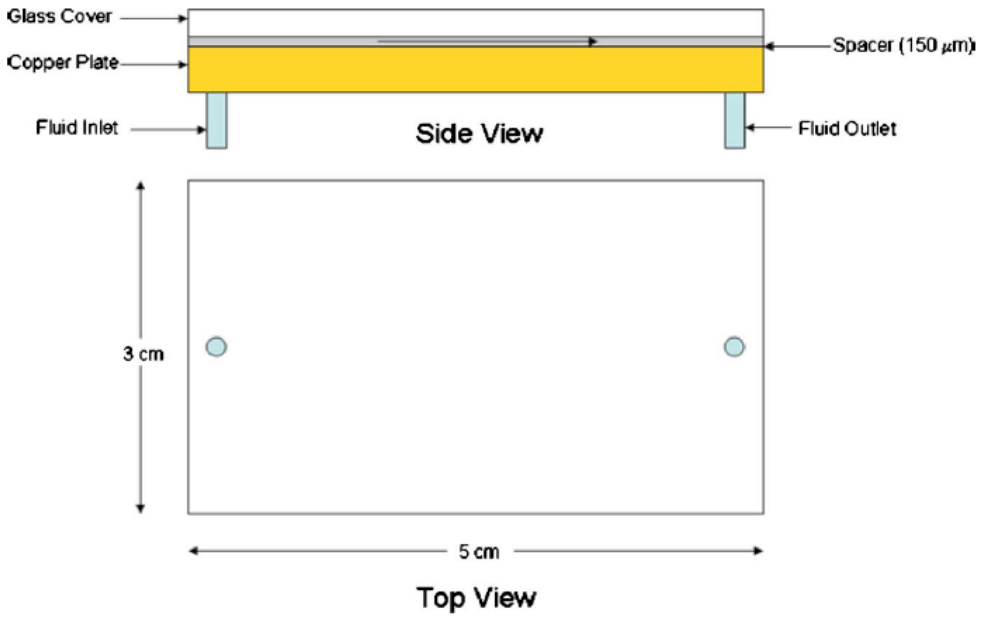

Fig 2.1

The flow rate is set to 42ml/hr via a syringe pump. The Set-up is a micro solar thermal collector, the micro geometry is selected to minimize the amount of nanofluid needed for the test. This set up is a type of Direct Absorption Solar Collector. Volume fraction and particle size are taken as the varying parameters. This report demonstrates efficiency improvement up to 5%.

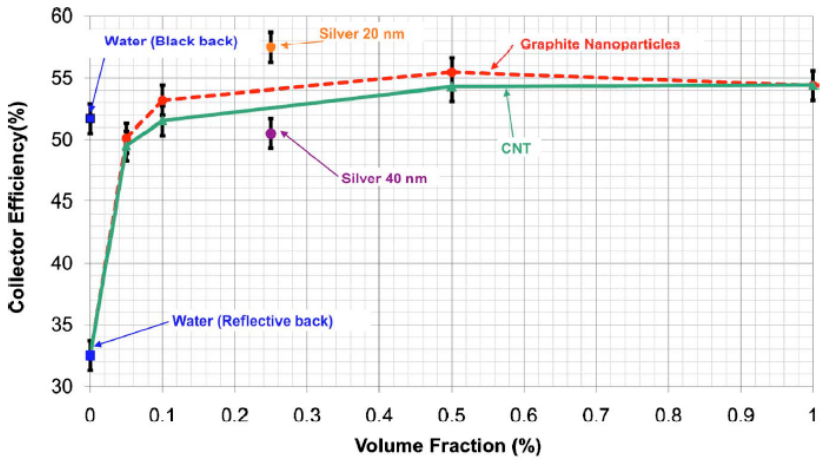

Fig 2.2

Efficiency is the ratio of usable thermal energy to the incident solar energy. In Fig 2.2 the variation of efficiency and volume fraction of nanoparticle in base fluid is shown. The small increase in volume fraction of nanoparticles results in a rapid efficiency enhancement. By

using 20nm silver nanoparticles an increase in efficiency of 5% can be achieved.

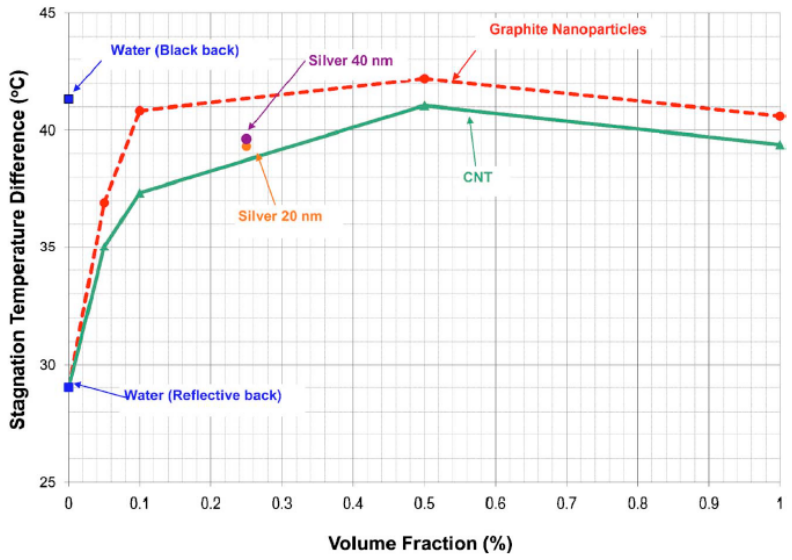

Fig 2.3

The plot between Temperature difference and volume fraction shows the same pattern. Again a rapid increases in the temperature difference as volume fraction of nanoparticles is increased.

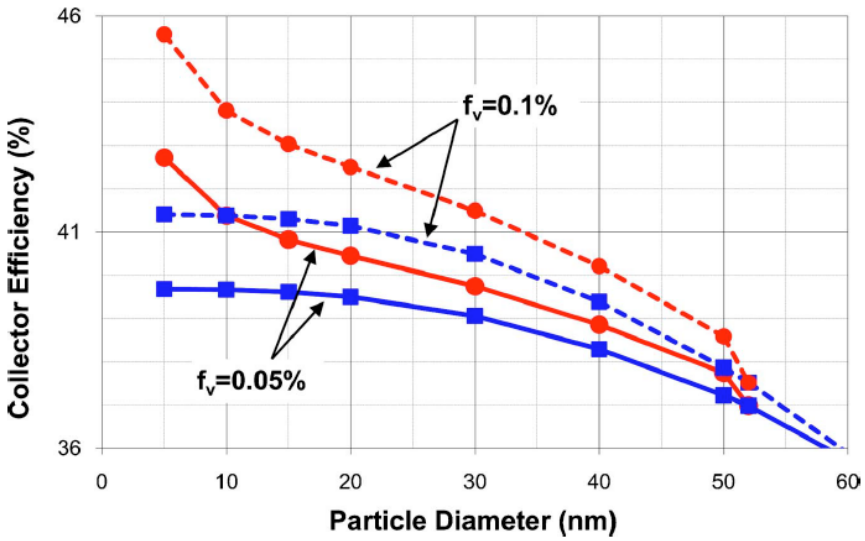

Fig.2.4 (Collector Efficiency as a function of Silver nanoparticle diameter and Volume fraction)

The above plot shows that the reduced size nanoparticle further leads to an even higher efficiency. In the plot squares shows the bulk properties and circles represents size dependent properties.

Tyagi H *et al.* [4]

This paper is the comparative study of the efficiency of direct absorber collector to that of a conventional flat plate collector using a nanofluid. In this study nanofluid contains water as the base fluid and aluminum as the nanoparticles. As the part of this study a 2-D heat transfer model is prepared and solved numerically.

Fig 2.5 is the schematic diagram of direct absorber solar collector. The main assumptions are:

1. The bottom wall is considered to be adiabatic.
2. The fluid is enclosed by a glass cover at the top.
3. The top surface is assumed to be exposed to the ambient atmosphere, so the heat losses are due to convection
4. Atmospheric absorption is neglected.

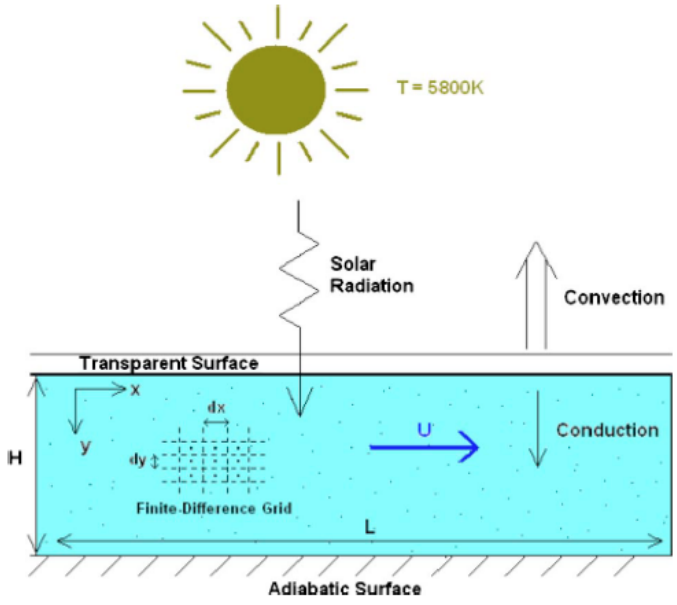

Fig 2.5

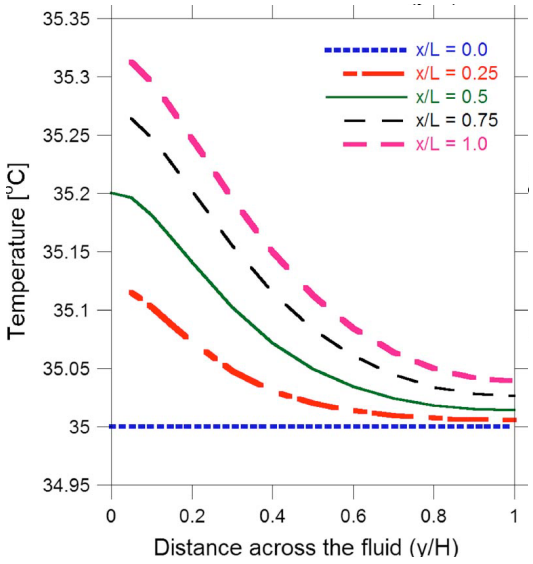

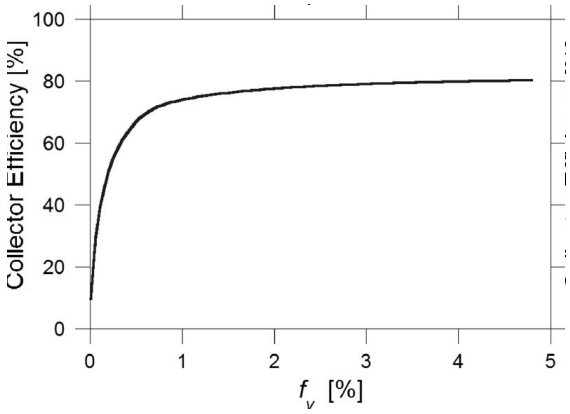

Fig 2.6 **Fig 2.7**

The plot in Fig 2.6 shows the expected pattern, the temperature variation of nanofluid increases as it flows through the collector. The temperature of upper layers is higher and lower for the layers at depth. For the plot particle size is 5nm and volume fraction is 0.8%.

Fig 2.7 shows collector efficiency as a function of volume fraction of nanoparticles for particle size d = 5nm, so it was observed that increment in volume fraction lead to an increase in sunlight passing through the collector, which, in turn, increases the collector efficiency.

Some more variations of collector efficiency with respect to other parameters are shown:

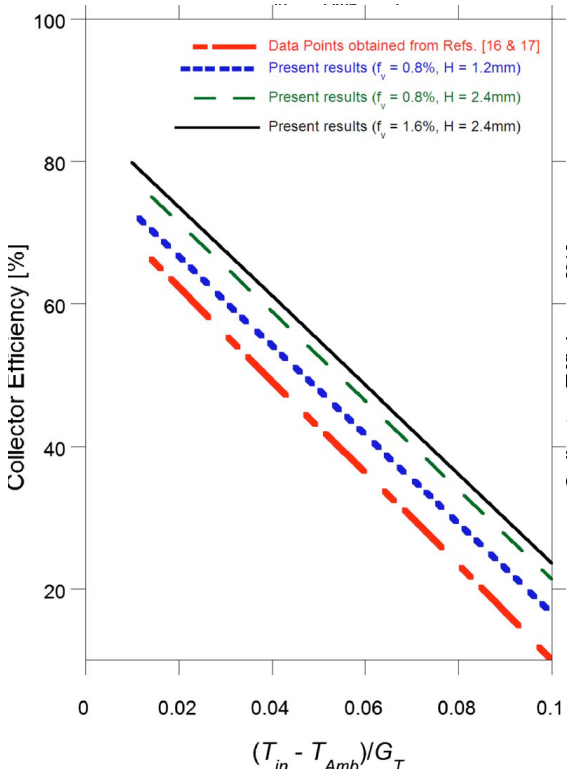

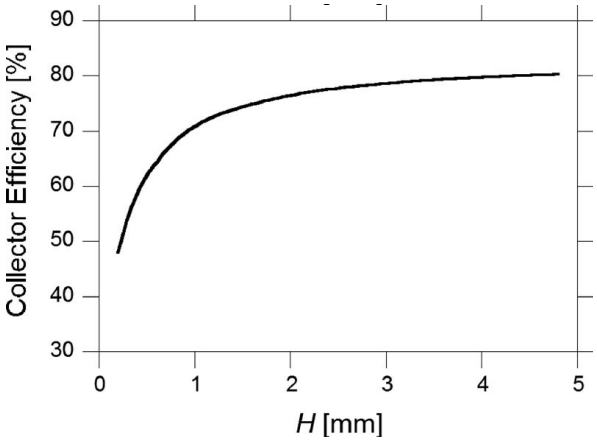

Fig 2.8 **Fig 2.9**

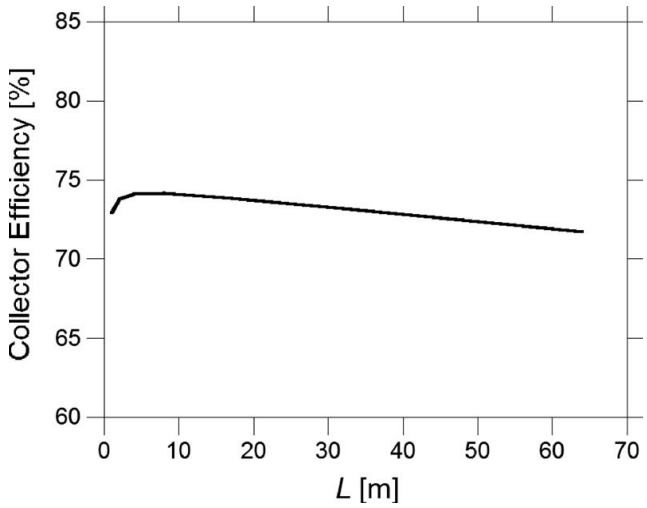

Fig 2.10

Fig 2.8 shows the comparison of the collector efficiency of a direct absorber collector and a conventional flat plate collector, the collector efficiency is shown as a function of T_{in}. In Fig 2.8.T_{in} is the inlet temperature T_{amb} is the ambient temperature and G_T is the solar irradiation, and size of the particle is 5nm.

In Fig. 2.9 and 2.10 the variation of efficiency with Height and length is plotted. In both cases Particle size is taken as D = 5nm and volume fraction as 0.8%. The plot in Fig2.10 can be explained as follows. Since the radiative energy decreases as the radiation passes through the collector, the top most layers gets heated the most. Simultaneously, heat is transferred to the lower layers of fluid, and some heat is lost via convection to the ambient. So, at very small collector lengths the temperatures are relatively low and hence convective heat loses are not significant. However, as the length is increased, after a certain point the relatively higher temperatures of the top layers contribute to higher convective losses, and thus the efficiency tends to gradually decrease with further increases in length.

Taylor R A *et al*. [5]

Talyor.R.A et al have investigated the nanofluid based concentrating solar collectors and performance was compared with conventional collectors. It is found that efficiency improvement was of the order of 5 – 10% for a nanofluid based receiver. This paper depicted that as solar power plant move to larger scale, nanofluids will have more potential. In this research work they have used a new receiver. The nanofluid used for this work consist of Therminol VP – 1 heat transfer oil as base fluid and graphite nanoparticles are dispersed in the base fluid. The volume fraction is used as 0.125% and 0.25%. As concentrating solar collector has a greater concentration ratio, so their efficiency is also higher.

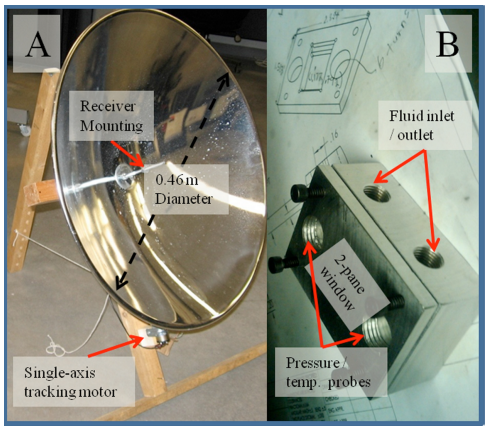

Fig 2.11 (A- reflective Dish, B- machined aluminum part with inlet and out let ports)

In Fig 2.11 part B is the receiver the gap between the plates is 1mm, and dimensions are as follows:

Area of receiver = 2cm x 2cm

Operating Temperature = 270˚C

Mass flow rate = 1 x 10^{-4} kg/s

Dish Concentration ratio = 400

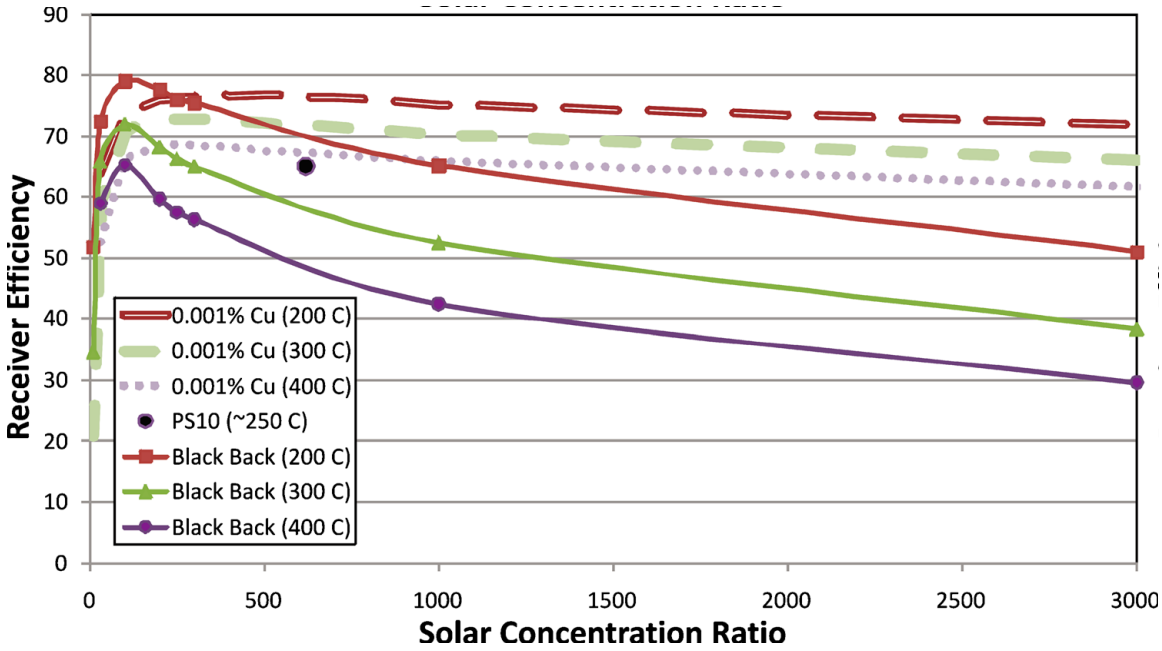

Fig 2.12

The Fig 2.12 shows model results for the pure base fluid i.e., nearly non absorbing with a selective surface "black backing" under similar receiver operating conditions. The results in Fig 2.12 illustrates that a nanofluid collector may operate more efficiently than a conventional surface solar collector under optimum conditions, up to 10% higher for solar concentration ratios in the range of 100–1000. As shown in the figure, the nanofluid and its operating conditions must be chosen carefully or the system may end up operating less efficiently.

This paper also describes the economic implications for the application of nanofluid in high flux solar collector. Nanofluids are not expected to be suitable for dish or trough solar power system one big reason for that is the high cost and economic factors.

Han Z. [6]

Heat transfer fluids have inherently low thermal conductivity that greatly limits the heat exchange efficiency. Liquid dispersions of nanoparticles, which have been termed “nanofluids”, exhibit substantially higher thermal conductivities than those of the corresponding base fluids. A nano - emulsification technique have been studied and developed to synthesize nanofluids. The thermal transport properties of nanofluids, including thermal conductivity, viscosity, heat capacity and heat transfer coefficient in convective environment were characterized and modeled.

Up to 126% and 20% increases in the effective heat capacity were experimentally found in water-in-FC72 nanoemulsions and indium-in-PAO nanofluids, respectively, due to the large amount of latent heat absorbed in phase transition from nanoparticles to nanodroplets and released in reverse transition. The results show that nanofluids possess improved thermal transport properties and it is believed that nanofluids have potential as next-generation advanced heat transfer fluids.

Zhou.K *et al*. [14]

This paper is about the manufacturing and characterization techniques of Copper Oxide – nanocrystals with different shapes. CuO-nanocrystals e.g. CuO nanoparticles, nanobelts and nanoplatelets can be synthesized by controlling some parameters. To investigate the characteristics of the crystals different techniques are used e.g. XRD, BET, TEM, SEM, HRTEM etc. XRD (X-Ray Diffraction) gives the confirmation of the CuO nanoparticles and determine the crystal structure. BET analysis gives the shape and surface area of nanoparticles. Transmission Electron Microscopy (TEM) gives information about the average size as well as the shape of the nanoparticles. Scanning Electron Microscopy (SEM) is used to predict the surface topography of the nanoparticles.

Kalogirou.S.A. [21]

This paper is a report on the classification of different types of solar collectors and their applications and this is followed by an optical, thermal and thermodynamic analysis of collectors and a description of the methods used to evaluate their performance.

The main applications of solar collectors include solar water heating, solar air heating, Space heating and cooling, refrigeration, thermal power systems, solar furnaces, desalination, steam generation systems, industrial process heating and chemistry applications.

Table 2.1: The comparison of various types of solar collectors

Collector type	Absorber type	Concentration ratio	Temperature Range
Flat plate	Flat	1	30 – 80
Evacuated Tube	Flat	1	50 – 200
Compound parabolic	Tubular	1 – 5	60 – 240
Linear Fresnal reflector	Tubular	10 – 40	60 - 250
Parabolic trough	Tubular	15 - 45	60 - 300
Cylindrical trough	Tubular	10 – 50	60 - 300
Parabolic Dish reflector	Point	100 – 1000	100 - 500
Heliostate	Point	100 - 1500	150 - 2000

Lenert.A. [27]

Surface receivers have low energy conversion efficiencies due to high losses at high temperatures, where as volumetric receivers show increase performance because solar radiation can be transferred in the fluid medium directly.

In this thesis, a modeling and experimental study to investigate the efficiency of nanofluid based solar receivers is presented. Effect of nanoparticle characteristics e.g. distribution and selectivity, as well as collector parameters (like absorbing height and concentration ratio) is evaluated. This study shows that volumetric receivers for solar collectors are more efficient at higher concentration and can achieve the power generation efficiencies up to 55% in these regimes.

Wang.X.Q. *et al.* [28]

This paper is a review of the recent research on fluid flow and heat transfer characteristics of nanofluids in forced and free convection flows. Convective heat transfer can be enhanced passively by changing flow geometry, boundary conditions, or by enhancing thermal conductivity of the fluid. By enhancing the thermal conductivity, heat transfer through the nanoparticles increases. Wang et al [30] measured the relative viscosity for Al_2O_3 – water and Al_2O_3 – ethylene glycol nanofluids, results showed similar trend of increase of relative viscosity with increased solid volume fraction for the two nanofluids. So, in turn heat transfer of nanofluid increases. Also past experiments shows higher value of convective heat transfer for nanofluids.

Yousefi.T, et al. [22]

The efficiency of a flat plate solar collector was investigated, having Al_2O_3 nanofluid as a working fluid, by Yousefi.T *et al*. The weight fraction of nanoparticles was taken as 0.2 % and 0.4 %. The nanoparticle size was 15nm. Yousefi.T *et al* also this experiment with and with out surfactant (Triton X – 100), and mass flow rate was 1 to 3 lit/min. The result shows that by using 0.2 % weight fraction nanofluid collector efficiency enhanced by 28.3%, also the surfactant causes an enhancement in heat transfer, by using surfactant the maximum enhanced efficiency is 15.63 %.

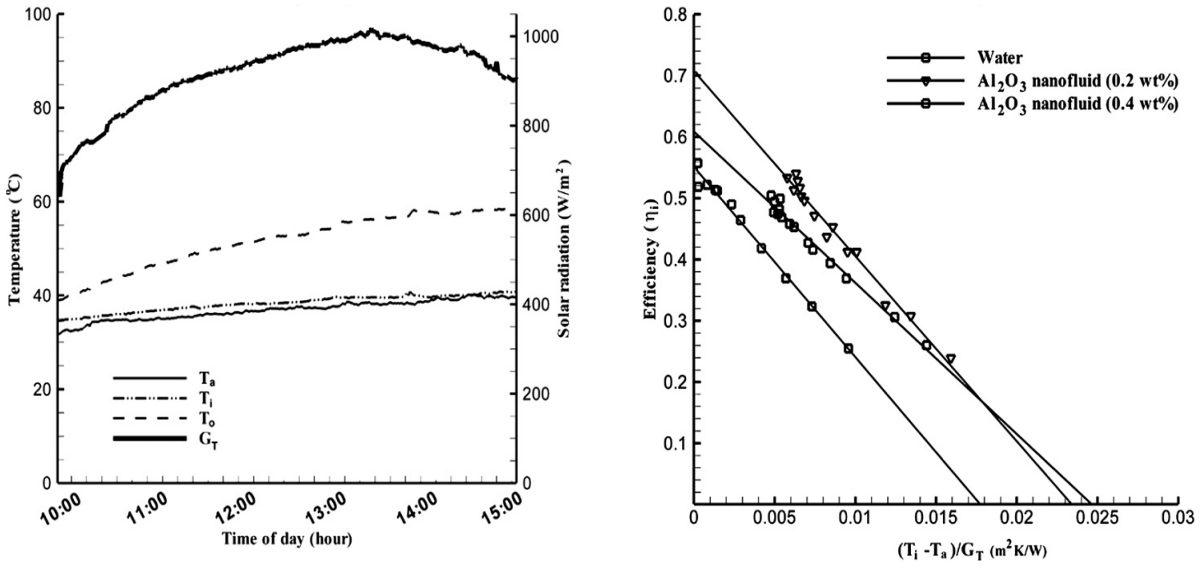

(a) (b)

Fig. 2.13 (a) Temperature (˚C) variation vs Time and Solar radiation (W/m²)

(b) Efficiency comparison for water and Al_2O_3 nanofluids

CHAPTER 3

OBJECTIVES

The efficiency of solar collector is mainly depends on the thermo – physical properties of the fluid which is absorbing the heat. So it has been found that the thermal properties (thermal conductivity, heat capacity, viscosity, etc.) of the fluid that is used to absorb the energy plays an important role to make the system more effective. By reviewing the past research, it has been concluded that conventional fluids can absorb heat up to a certain limit which, in turn, limits the efficiency of solar collector, where as recently developed new class of fluids called "Nanofluids" possesses very good thermal properties. So these nanofluids can be used in solar collectors in order to improve its performance. So this thesis is mainly focused on performance evaluation of solar collectors using nanofluids.

The main objectives of this Experimental work are as follows:

1. To investigate the collector efficiency throughout the day using water.
2. To investigate the collector efficiency throughout the day (hourly) using $CuO - H_2O$ nanofluid.
3. To investigate the collector efficiency with varying volume fraction of nanoparticles.
4. To examine the temperature variation throughout the day (hourly).
5. To compare the performance of solar collector for nanofluid and water.

CHAPTER 4

METHEDOLOGY

In this chapter, the procedure to evaluate the objectives is discussed. Main steps of methodology are as follows:

a. ASHRAE Standards 93-77for the testing of solar collectors.
b. Experimental Set-up
c. Direct absorption method is adopted for the experiment
d. Nanofluid used

Base fluid – Water

Nanoparticles – Copper Oxide (CuO)

1.1 ASHRAE Standards 93 – 77 [11, 12]

Following ASHRAE standards are used for this study.

1. For the measurement of solar radiation in the plane of the collector, a pyranometer as classified by the World Meteorological Organization should be used.
2. Data should be taken during the middle of the day, preferably when the solar incident angle is less then 30˚.
3. A series of tests should be conducted, each of which determines the average efficiency of a 5 – min period.
4. In computing efficiency, the gross frontal area is used instead of aperture area.
5. The efficiency curve is drawn by plotting efficiency is as a function of the difference between the inlet fluid temperature and the ambient temperature divided by the incident solar radiation.
6. The collector is required to undergo a preconditioning test prior to the start of thermal tests. The collector must be exposed for three consecutive days with no fluid passing through it and with the mean incident solar radiation measured in the plane of the collector aperture exceeding 17,000 kJ/m^2 days.

7. Before the efficiency test, the time constant is determined. The time constant test determines the transient thermal properties of the collector.
8. The entire group of test may be made in doors using a solar simulator if desired
9. After the efficiency tests are completed, a series of tests is conducted to determine the collector's incident angle modifier. The collector's incident angle modifier test consists of a series of efficiency determinations for a range of incident angles, with the inlet fluid temperature of the collector equal to the ambient temperature.
10. The inlet fluid temperature to the collector must be adjusted and controlled to a desired value or constant.
11. On any given day, data is recorded under steady state conditions for fixed values of mass flow rate and inlet temperature.

1.2 Experimental Set – Up

The model for the test apparatus is shown in Fig.4.1. The mini channel geometry is selected to minimize the amount of nanofluid needed for the test. In this set-up CuO – H_2O based nanofluid is used. An Infusion Set is used to have a constant flow of nanofluid.

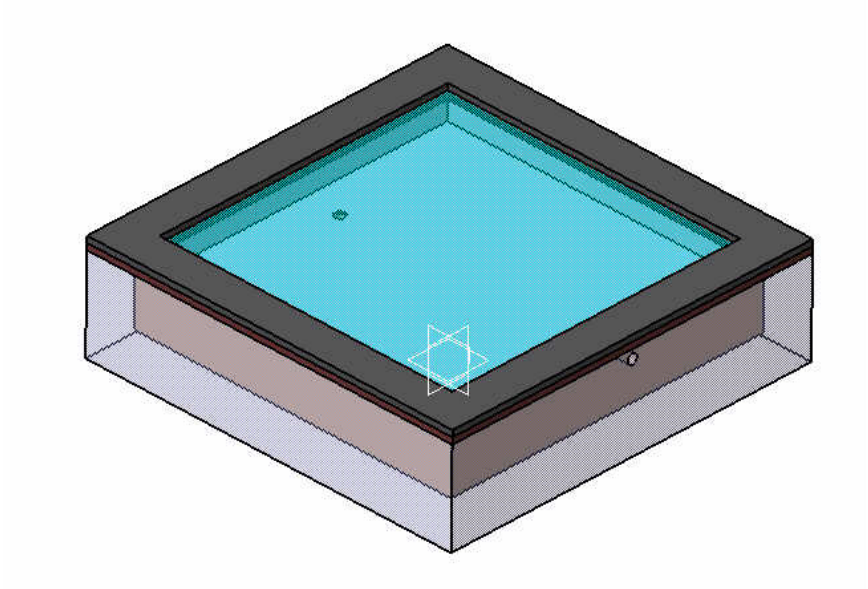

Fig. 4.1 (3D Model of the experimental set-up)

The collector glazing is a low reflectance glass. In the apparatus, copper plate is black painted to increase the absorption capacity of the plate. This is a volume absorption system rather than a surface absorption system, as the solar energy is directly absorbed with in the fluid volume. This is also called Direct Absorption Solar Collector.

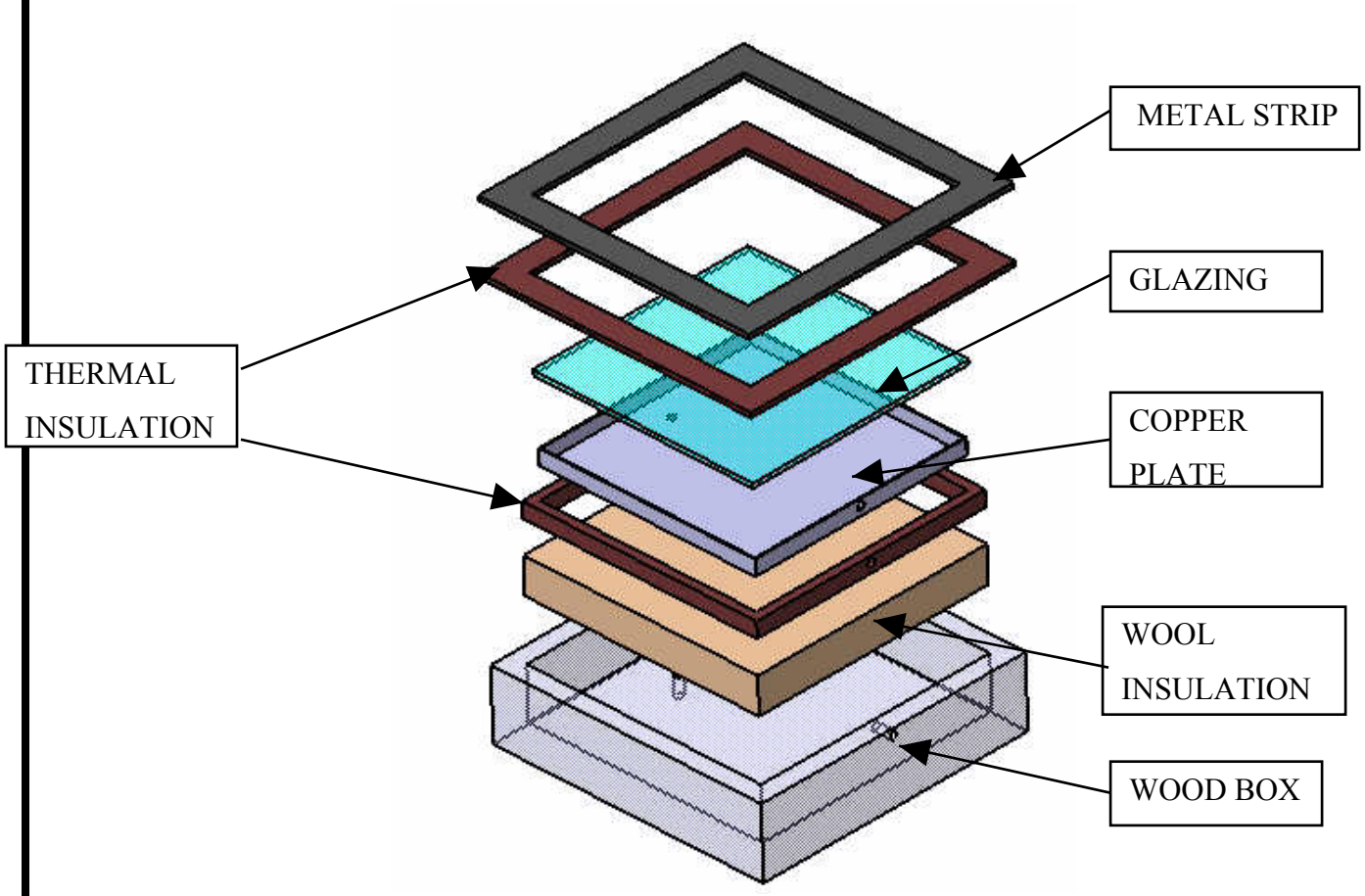

Fig. 4.2 (exploded view of Apparatus)

Nanofluid flows over the copper plate. Thermocol and glass wool is used for the thermal insulation. Thermocol insulation is given between the gap of copper plate and wood box. Wool insulation is given at the bottom of the copper plate to prevent the heat loss.

The dimensions of the apparatus are shown in Fig.4.3

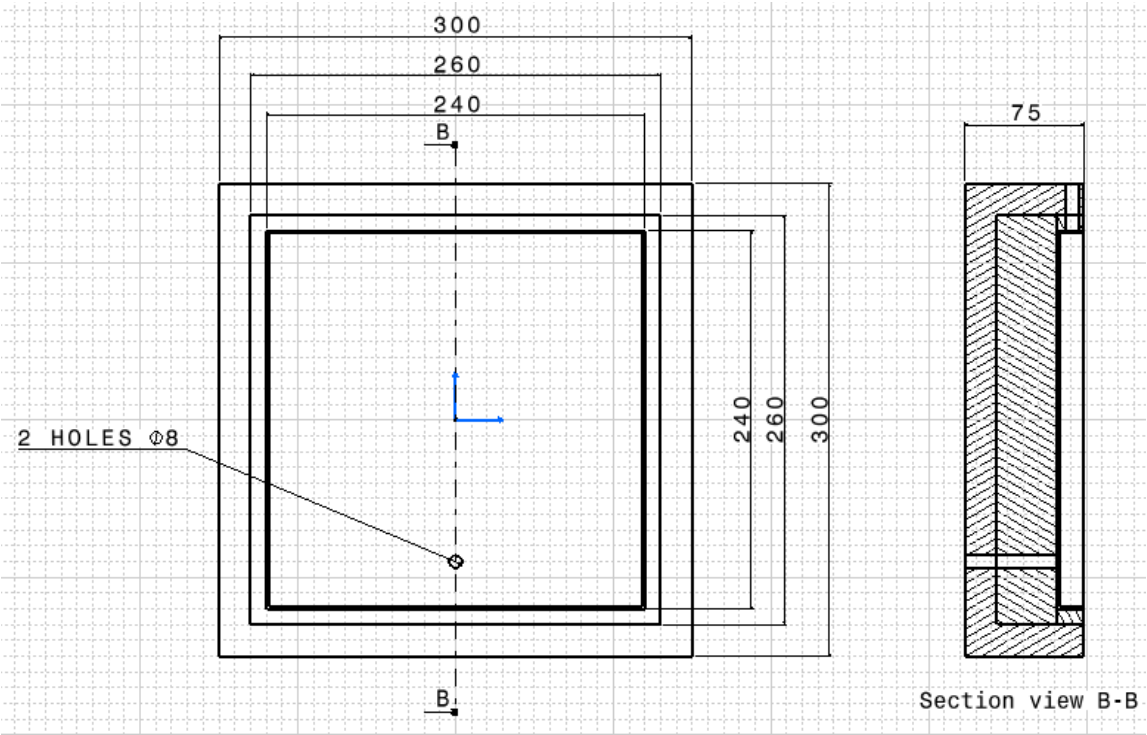

Fig. 4.3

Fig. 4.4

4.3 Preparation of Nanofluids

(i) Synthesis of Nanoparticles [19]

CuO nanoparticles are synthesized by precipitation method. In this method Cupric Nitrate [$Cu(NO_3)_2.3H_2O$] is dissolved in distilled water then Sodium Carbonate [Na_2CO_3 (1M)] is mixed with the above solution to adjust the pH value of the solution to 10. The product is then aged with the mother liquor at room temperature for 12h [19]. The resultant product is then filtered, washed with distilled water using centrifuge. After washing the product is dried at 60˚C for 24 hrs and then calcined in Muffel furnace at 350˚C for 4 hr.

Fig 4.5 (CuO nanoparticle prepared at laboratory)

(ii) Structural Characterization

Structural Characterization of nanoparticles can be done by using techniques such as BET, XRD, SEM, TEM, and HRTEM. As this research work is more concerned about the application of nanofluids so XRD analysis is done for the authentication of nanoparticles. XRD for two samples (Purchased and manufactured at the laboratory) are shown.

Purchased Sample XRD:

Company Name: Reinste Nano Venture Pvt. Ltd.

Cooper Oxide

CuO – Nanoparticle Powder, purity: >99%

Particle Shape: Spherical

Average particle size: 40nm

Specific surface: >10 m^2/g

Bulk Density: 0.8 g/cm^3

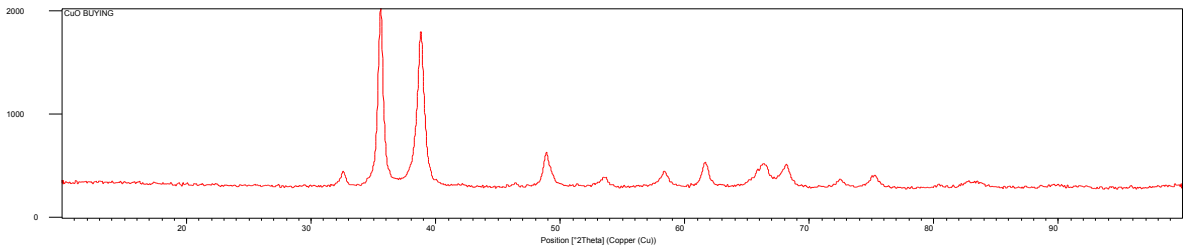

Fig. 4.6

Prepared at Laboratory XRD:

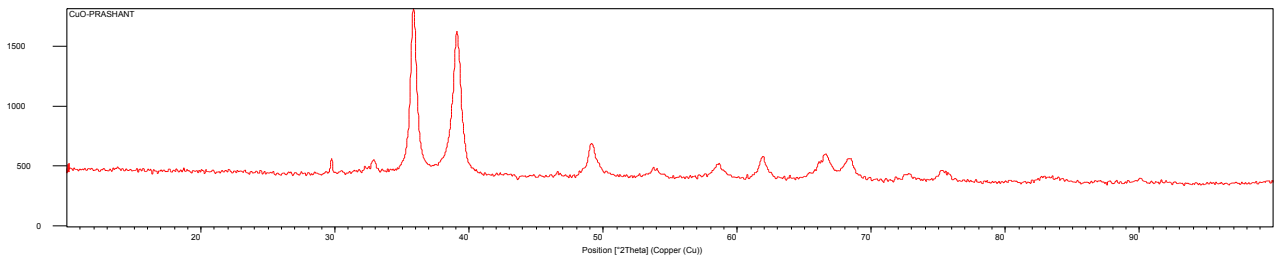

Fig. 4.7

For the details of XRD analyses refer Appendix.

(iii)Sonication [18]

To prepare the CuO nanofluid, there is a need to determine the weight of CuO for different concentration. The weight of CuO can be evaluated by using the standard expression.

$$\varphi = V_P / V_{eff}$$

Where, $V_P = W_P / \rho_P$

$V_{eff} = V_P + V_f$, $V_f = W_f / \rho_f$

Quantity of Base fluid (Water), $V_f = 500ml$

Density of CuO particles, $\rho_P = 6.31$ gm/cm^3

Density of water, $\rho_f = 1000$ kg/m^3

Table 4.1: Shows the weight of CuO particles to prepare the nanofluid of different concentration.

Φ	0.005	0.05
W_p (gms)	0.157	1.57

Now, CuO particles of required amount put into a container, and then water is poured into it. The solution then put on the sonicator, and sonication is done for one and half hour, after sonication the required nanofluid solution is ready for the application. The sonicator is used shown in Fig. 4.7 is a probe type sonicator. The samples of prepared nanofluids for two concentrations are shown in Fig. 4.8.

Fig. 4.8 Oscar Ultra Sonicator (Probe Type)

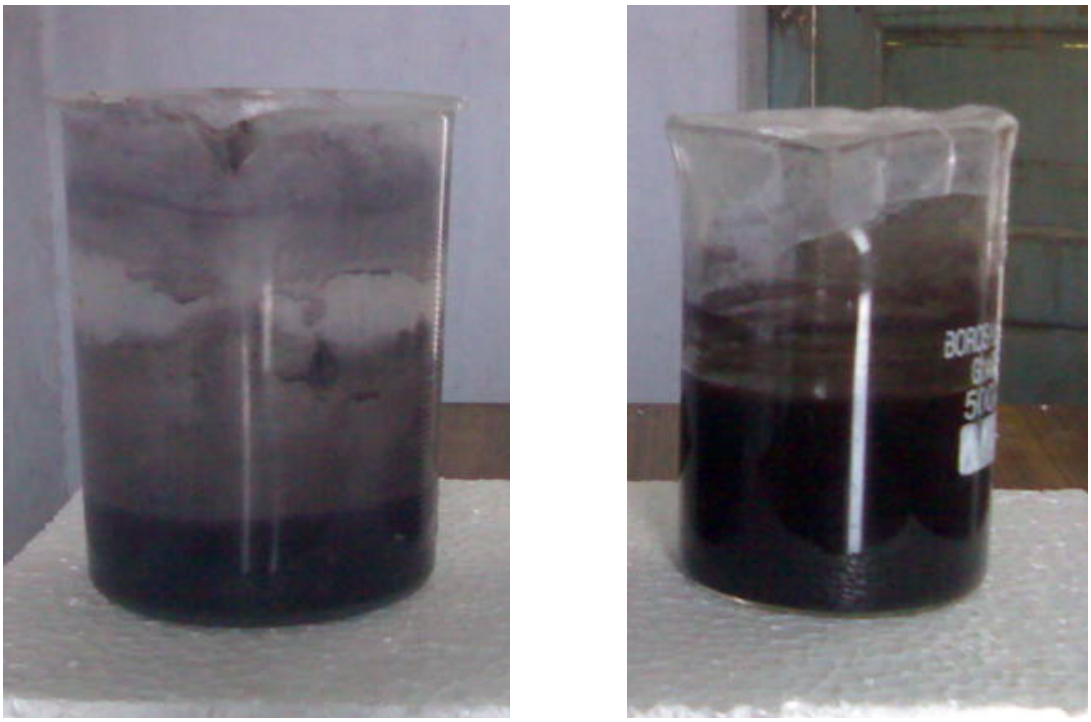

(a) (b)

Fig. 4.9 (a) (CuO-H2O) Nanofluid (with 0.005% volume Concentration)

(b) (CuO-H2O) Nanofluid (with 0.05% volume Concentration)

4.4 Instruments

Various types of instruments are used for this study as follows:

1) Pyranometer

2) Digital Thermometer

3) Infusion Set

Pyranometer [10]

A pyranometer is an instrument which measures total or global radiation over a hemispherical field of view. It is a sensor that is designed to measure the solar radiation flux density (in watts per metre square) from a field of view of 180 degrees. The name pyranometer is originated from greek word "pyr" meaning "fire" and "ano" meaning "above sky". The pyranometer measures both beam as well as diffused radiations.

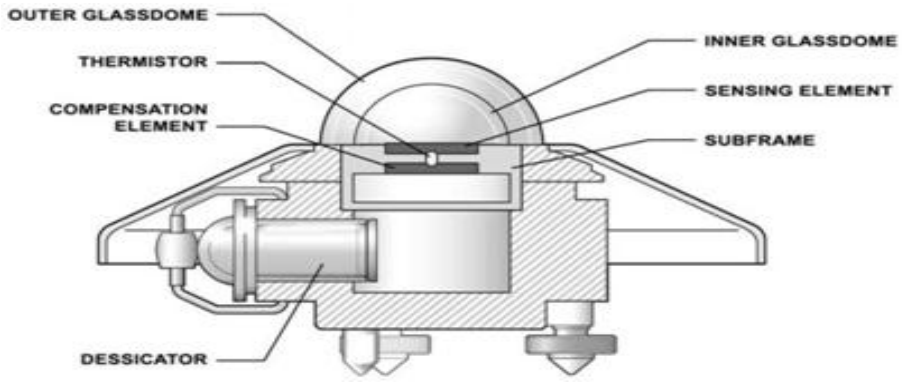

Fig. 4.10 [16]

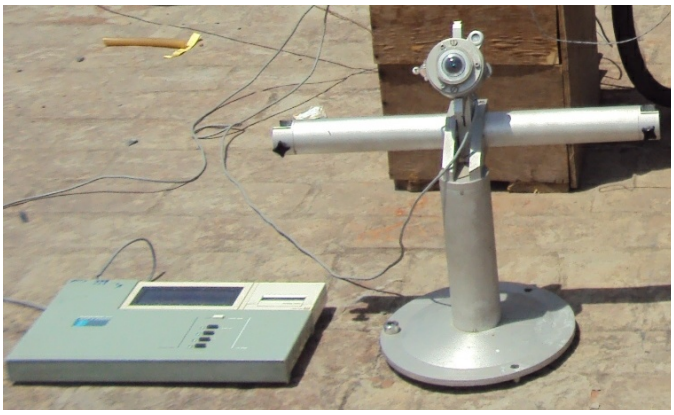

Fig. 4.11 (Kipp & Zonen Pyranometer)

To make a measurement of irradiance, the sensitive surface of pyranometer consists of a circular, blackened multi junction thermopile whose cold junctions are electrically insulated from the basement. The temperature difference between hot and cold junctions is a function of the radiation falling on the surface. A pyranometer produces voltage as a function of the incident radiation, from the thermopile detectors. The black coating on the thermopile sensor absorbs the solar radiation. This radiation is converted to heat. The heat flows through the sensor to the pyranometer housing. The thermopile sensor generates a voltage output signal that is proportional to the solar radiation.

The pyranometer used for the measurement of the solar radiation is shown in Fig. 4.6.

Company Name: KIPP & ZONEN

Model No. : CMP – 11

Operating Temperature Range: -40˚C to +80˚C

Max. Solar Irradiance Measurement: 4000 W/m^2

Field of view: 180˚C

Infusion Set

This instrument is used in medical treatments. This instrument is used for low mass flow rate. The fluid flow is under gravity effect.

According to the specification 20 drops of fluid makes 1ml ($\pm$ 0.1ml).

So, For 60 ml/hr

No. of drops = 20 / min.

For 80 ml/hr

No. of drops = 27 / min.

For 100 ml/hr

No. of drops = 33 / min.

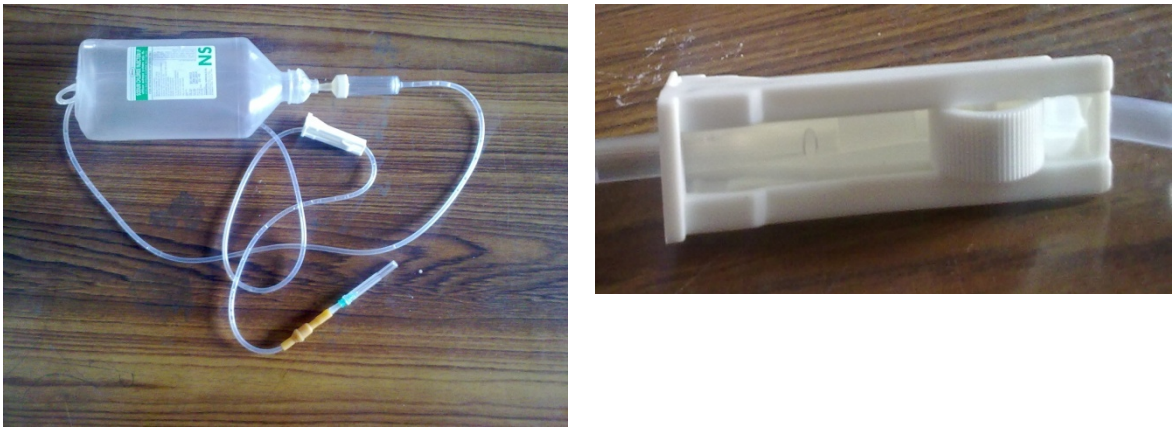

(a) (b)

Fig.4.12 (a) Infusion Set, (b) Flow control mechanism

CHAPTER 5

RESULTS AND DISCUSSIONS

This Chapter represents a detailed description of the result and their analysis, which were obtained after performing the experiment. The chapter contains the calculation for solar collector followed by its overall efficiency variation and effect of nanofluids on the performance of flat plate solar collectors.

5.1 Solar Collector Performance Calculations

The experimental efficiency of the solar collector [7] is:

General Expressions:

Heat Absorbed by Solar Collector

$$Qa = m\ C\ (T_2 - T_1) \times 1000\ W \quad \text{.....1}$$

Total Average Solar Radiation fall on Solar Collector

$$Qi = G_T A C_r \quad \text{.....2}$$

$$\eta = m\ C\ (T_2 - T_1) / G_T A C_r \quad \text{.....3}$$

$$m = \rho \times v \quad \text{.....4}$$

Expressions for nanofluids

$$\eta = m\ C_{eff} (T_2 - T_1) / G_T A C_r \quad \text{..... 5}$$

$$m = \rho_{eff} \times v \quad \text{.....6}$$

$$\rho_{eff} = (1 - \varphi_p)\ \rho_f + \varphi_p \rho_p \quad \text{..... .....7}$$

$$\varphi_p = V_p / (V_p + V_f) \quad \text{.....8}$$

$$C_{eff} = \{(1 - \varphi_p)\ \rho_f\ c_f + \varphi_p \rho_p c_p\} / \rho_{eff} \quad \text{.....9}$$

Table 5.1: Measurement of Solar radiation using Pyranometer (W/m^2)

Time	5/5/2012	6/5/2012	7/5/2012	10/5/2012	13/5/2012	18/5/2012	20/5/2012	21/5/2012	24/5/2012
10:00 AM	590	580	600	588	595	610	585	605	596
11:00 AM	685	690	725	690	690	805	705	712	708
12:00 PM	805	810	835	815	825	755	817	815	840
1:00 PM	965	965	980	975	960	810	978	925	985
2:00 PM	910	905	915	865	855	625	865	860	875
3:00 PM	803	805	820	790	778	545	795	790	796

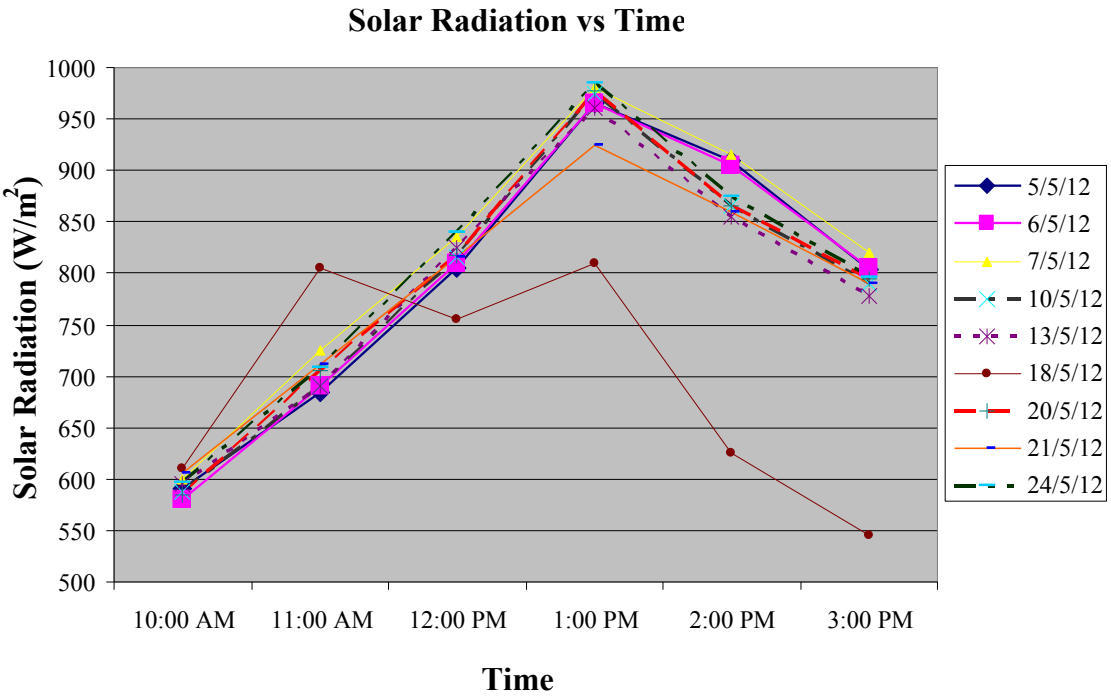

Fig. 5.1 (Solar Radiation Variation with time on different days)

Solar Collector Area 'A' = 0.0576 m^2

Total Solar radiation on the Solar collector area = A x G_T (W/m^2)

Table 5.2: Total Solar Radiation (W) on the solar collector area

Time	5/5/2012	6/5/2012	7/5/2012	10/5/2012	13/5/2012	18/5/2012	20/5/2012	21/5/2012	24/5/2012
10:00 AM	33.984	33.408	34.56	33.8688	34.272	35.136	33.696	34.848	34.3296
11:00 AM	39.456	39.744	41.76	39.744	39.744	46.368	40.608	41.0112	40.7808
12:00 PM	46.368	46.656	48.096	46.944	47.52	43.488	47.0592	46.944	48.384
1:00 PM	55.584	55.584	56.448	56.16	55.296	46.656	56.3328	53.28	56.736
2:00 PM	52.416	52.128	52.704	49.824	49.248	36	49.824	49.536	50.4
3:00 PM	46.2528	46.368	47.232	45.504	44.8128	31.392	45.792	45.504	45.8496

As per ASHRAE standard, for this experiment inlet fluid temperature of the solar collector is assumed as 29˚C. Correction factor 'C_r' for the collector is taken as 0.92. Correction factor is introduced to compensate the heat lost from the collector via. convection, dust and wind.

1.1.1 Solar collector performance using Water

For Water

Density $\rho = 1000$ kg/m^3

Specific Heat $C_P = 4.187$ KJ/KgK

Mass flow rate $m = \rho \times v$

Table 5.3: Mass Flow Rate

Vol. flow rate (ml/hr)	Mass flow rate (Kg/sec.)
60	1.666×10^{-5}
80	2.222×10^{-5}
100	2.777×10^{-5}

Table 5.4: Temperature Readings for Water

Time	Temperature Inlet	Temperature Outlet			Temperature Difference		
		60 ml/hr (5/5/12)	80 ml/hr (6/5/12)	100 ml/hr (7/5/12)	60 ml/hr (5/5/12)	80 ml/hr (6/5/12)	100 ml/hr (7/5/12)
10:00 AM	29	57.9	56.1	58.2	28.9	27.1	29.2
11:00 AM	29	61.2	60.4	60.6	32.2	31.4	31.6
12:00 PM	29	63.5	65.2	64.7	34.5	36.2	35.7
1:00 PM	29	71.4	69.6	69.2	42.4	40.6	40.2
2:00 PM	29	70.8	68.7	68.1	41.8	39.7	39.1
3:00 PM	29	64.7	67.5	66.3	35.7	38.5	37.3

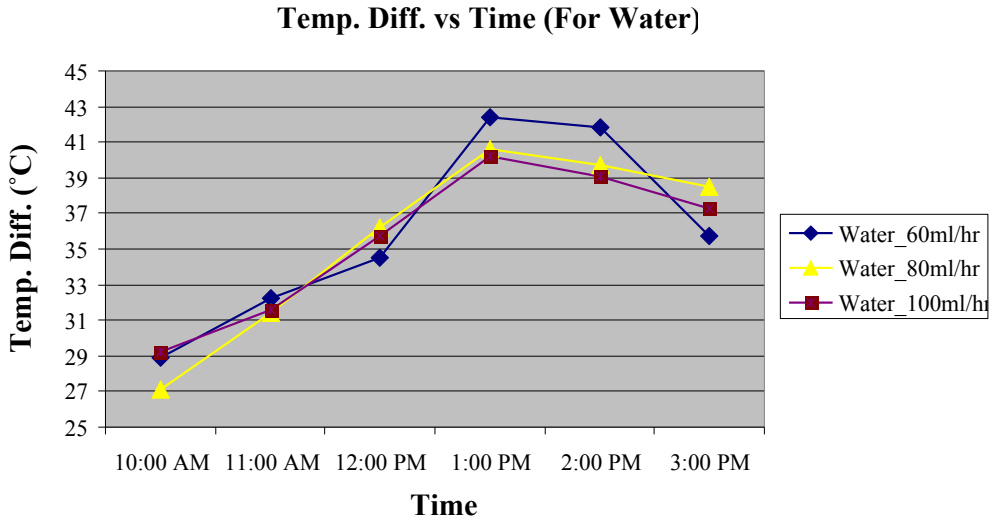

Fig. 5.2

Table 5.5: Efficiency for collector using Water (For different mass flow rate)

Time	Total Solar Radiation 'W'			Heat Absorbed 'W'			Efficiency 'η' %		
	5/5/2012	6/5/2012	7/5/2012	60 ml/hr (5/5/12)	80 ml/hr (6/5/12)	100 ml/hr (7/5/12)	60 ml/hr (5/5/12)	80 ml/hr (6/5/12)	100 ml/hr (7/5/12)
10:00 AM	33.984	33.408	34.56	2.01674	2.5215	3.3961	6.45041	8.20391	10.68117
11:00 AM	39.456	39.744	41.76	2.247	2.9215	3.6752	6.19016	7.98999	9.56605
12:00 PM	46.368	46.656	48.096	2.4075	3.3682	4.1521	5.64365	7.84698	9.383633
1:00 PM	55.584	55.584	56.448	2.9588	3.7776	4.6754	5.78599	7.38717	9.002899
2:00 PM	52.416	52.128	52.704	2.9169	3.6938	4.5475	6.04881	7.70219	9.378671
3:00 PM	46.2528	46.368	47.232	2.4913	3.5822	4.3381	5.85464	8.39738	9.983329

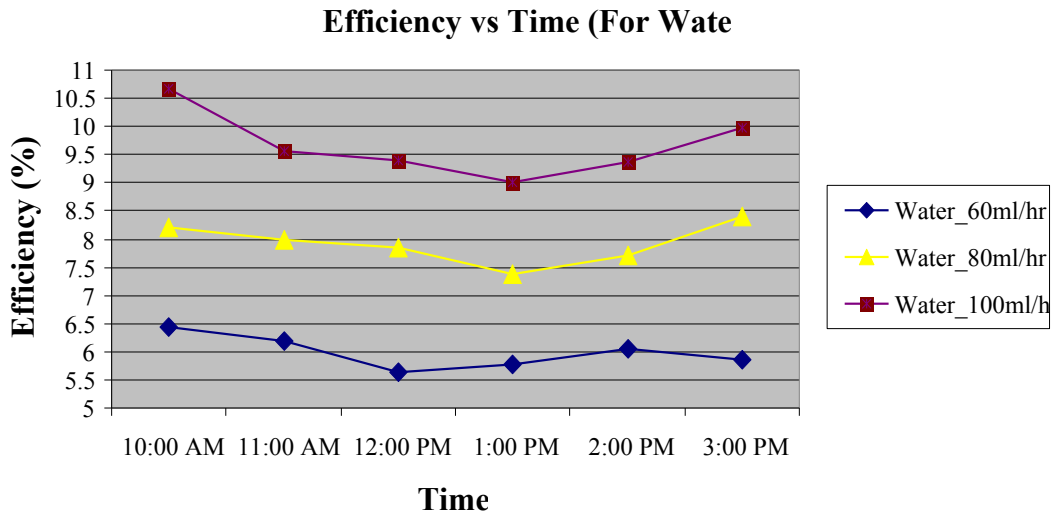

Fig. 5.3

In Fig. 5.2 and 5.3 variation of temperature difference and efficiency are plotted. It can be seen from these plots as the mass flow rate through the DASC increases temperature difference decreases slightly but there is a higher change in the efficiency, its reason may be that the percentage change of temperature difference is much lesser then the percentage change of mass flow rate of water. Temperature difference increases till 1:00 PM and then decreases, where as the collector efficiency has a lowest value at 1:00 PM. It is because the rate of heat absorption capacity is lesser then the rate of increase in solar irradiation falling on the earth.

1.1.2 Solar collector performance using CuO nanofluid (φ_P = 0.05%):

For CuO (φ_P = 0.05%) Nanofluid

Density of Base fluid (water) $\rho_f = 1000$ kg/m^3

Particle Density of CuO nanoparticle $\rho_P = 6310$ kg/m^3

Density of Nanofluid $\rho_{eff} = 1265.5$kg/m^3

Specific Heat of Base fluid (water) C = 4.187 KJ/KgK

Specific Heat of CuO nanoparticle $C_P = 0.5318$ KJ/KgK

Specific Heat of CuO nanofluid $C_{eff} = 3.2757$ KJ/KgK

Mass flow rate $m = \rho \times v$

Table 5.6: Mass Flow Rate

Vol. flow rate (ml/hr)	Mass flow rate (Kg/sec.)
60	2.11×10^{-5}
80	2.812×10^{-5}
100	3.515×10^{-5}

Table 5.7: Temperature Readings for CuO Nanofluid (φ = 0.05%)

Time	Temperature Inlet	Temperature Outlet			Temperature Difference		
		60 ml/hr (10/5/12)	80 ml/hr (13/5/12)	100 ml/hr (18/5/12)	60 ml/hr (10/5/12)	80 ml/hr (13/5/12)	100 ml/hr (18/5/12)
10:00 AM	29	57.1	56.5	57.2	28.1	27.5	28.2
11:00 AM	29	63.5	62.4	66.3	34.5	33.4	37.3
12:00 PM	29	64.4	67.4	61.7	35.4	38.4	32.7
1:00 PM	29	73.7	70.9	64	44.7	41.9	35
2:00 PM	29	69.7	65.8	57.2	40.7	36.8	28.2
3:00 PM	29	66.8	63.6	55.5	37.8	34.6	26.5

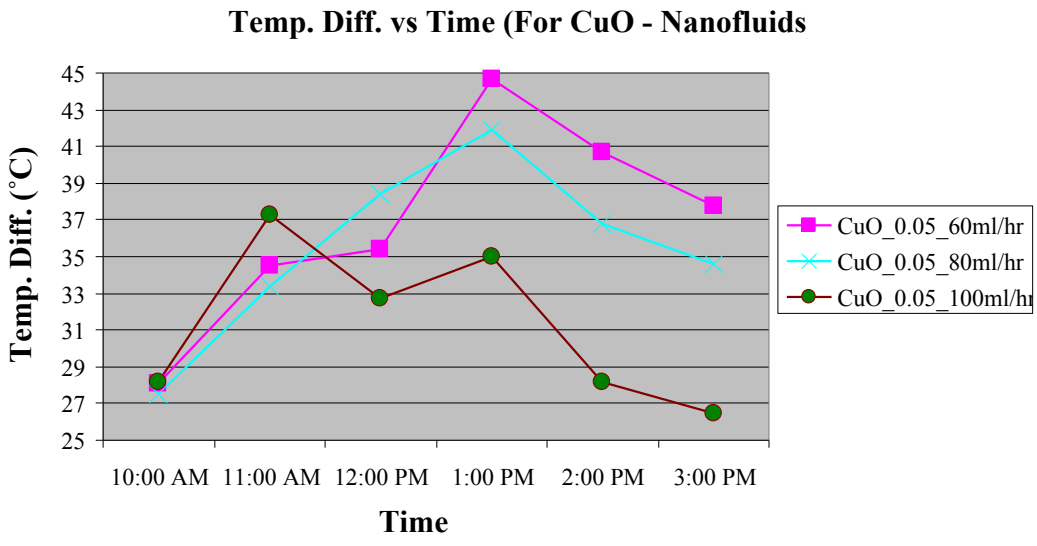

Fig. 5.4

Table 5.8: Efficiency for collector using CuO Nanofluid, φ_P = 0.05%, (For different mass flow rate)

Time	Total Solar Radiation 'W'			Heat Absorbed 'W'			Efficiency 'η' %		
	10/5/2012	13/5/2012	18/5/2012	60 ml/hr (10/5/12)	80 ml/hr (13/5/12)	100 ml/hr (18/5/12)	60 ml/hr (10/5/12)	80 ml/hr (13/5/12)	100 ml/hr (18/5/12)
10:00 AM	33.8688	34.272	35.136	1.9414	2.5333	3.2472	6.23056	8.03451	10.04544
11:00 AM	39.744	39.744	46.368	2.3836	3.0768	4.2951	6.51889	8.41472	10.06855
12:00 PM	46.944	47.52	43.488	2.4458	3.5374	3.7654	5.66308	8.09133	9.411392
1:00 PM	56.16	55.296	46.656	3.0883	3.8598	4.0302	5.97729	7.58723	9.389258
2:00 PM	49.824	49.248	36	2.8119	3.39	3.2472	6.13442	7.4821	9.804348
3:00 PM	45.504	44.8128	31.392	2.6116	3.1873	3.0514	6.23834	7.73095	10.56556

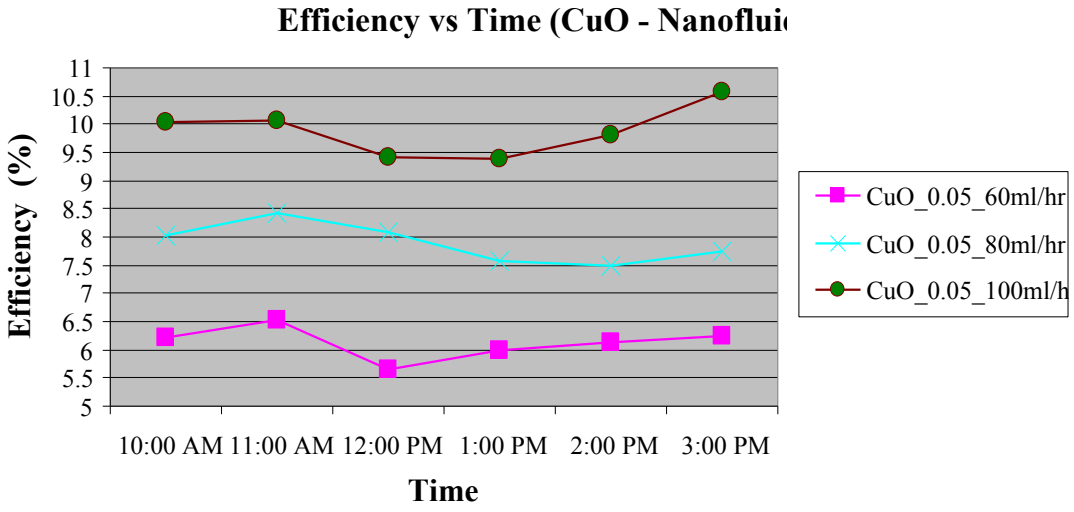

Fig. 5.5

Variation of temperature difference and collector efficiency for CuO nanofluid of volume fraction 0.05% throughout the day is shown in Fig. 5.4 and 5.5. It is clear that the efficiency of the collector has a greater value by using CuO nanofluid then water. It is because of the higher thermal properties (thermal conductivity, Heat transfer co-efficient) and higher thermo physical properties (density, viscosity, specific heat capacity) of CuO nanoparticles.

1.1.3 Solar collector performance using CuO nanofluid (φ_P = 0.005%):

For CuO (φ_P = 0.005%) Nanofluid

Density of Base fluid (water) $\rho_f = 1000$ kg/m^3

Particle Density of CuO nanoparticle $\rho_P = 6310$ kg/m^3

Density of Nanofluid $\rho_{eff} = 1026.55$ kg/m^3

Specific Heat of Base fluid (water) C = 4.187 KJ/KgK

Specific Heat of CuO nanoparticle $C_P = 0.5318$ KJ/KgK

Specific Heat of CuO nanofluid $C_{eff} = 4.0746$ KJ/KgK

Mass flow rate $m = \rho \times v$

Table 5.9: Mass Flow Rate

Vol. flow rate (ml/hr)	Mass flow rate (Kg/sec.)
60	1.711×10^{-5}
80	2.281×10^{-5}
100	2.851×10^{-5}

Table 5.10: Temperature Readings for CuO Nanofluid (φ = 0.005%)

Time	Temperature Inlet	Temperature Outlet			Temperature Difference		
		60 ml/hr (20/5/12)	80 ml/hr (21/5/12)	100 ml/hr	60 ml/hr (20/5/12)	80 ml/hr (21/5/12)	100 ml/hr (24/5/12)
10:00 AM	29	57.9	58.1	57.2	28.9	29.1	28.2
11:00 AM	29	63.9	63.5	61.6	34.9	34.5	32.6
12:00 PM	29	66.8	66.8	66.5	37.8	37.8	37.5
1:00 PM	29	72.3	69.9	71.9	43.3	40.9	42.9
2:00 PM	29	68.8	67.9	67.2	39.8	38.9	38.2
3:00 PM	29	67.3	65.8	65.3	38.3	36.8	36.3

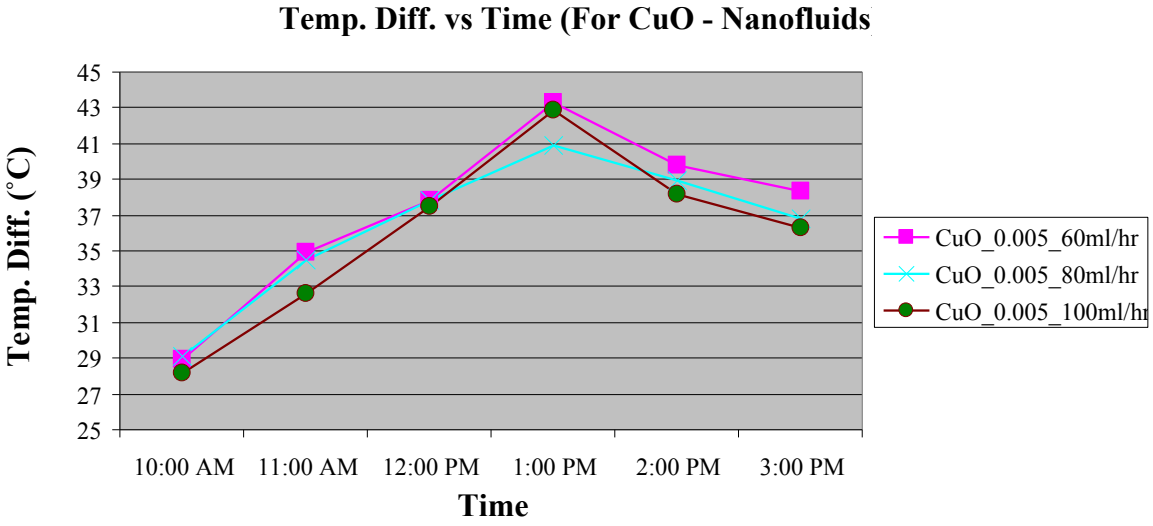

Fig. 5.6

Table 5.11: Efficiency for collector using CuO Nanofluid, φ_P = 0.005%, (For different mass flow rate)

Time	Total Solar Radiation 'W'			Heat Absorbed 'W'			Efficiency 'η' %		
	20/5/2012	21/5/2012	24/5/2012	60 ml/hr (20/5/12)	80 ml/hr (21/5/12)	100 ml/hr (24/5/12)	60 ml/hr (20/5/12)	80 ml/hr (21/5/12)	100 ml/hr (24/5/12)
0:00 AM	33.696	34.848	34.3296	2.0147	2.7049	3.2765	6.49897	8.43695	10.37418
1:00 AM	40.608	41.0112	40.7808	2.433	3.2068	3.7877	6.51242	8.49927	10.0956
2:00 PM	47.0592	46.944	48.384	2.6352	3.5135	4.3571	6.08669	8.13527	9.788315
1:00 PM	56.3328	53.28	56.736	3.0186	3.8017	4.9845	5.82447	7.75579	9.549377
2:00 PM	49.824	49.536	50.4	2.7746	3.6158	4.4384	6.05305	7.93406	9.572119
3:00 PM	45.792	45.504	45.8496	2.67	3.4206	4.2177	6.33773	8.17081	9.998902

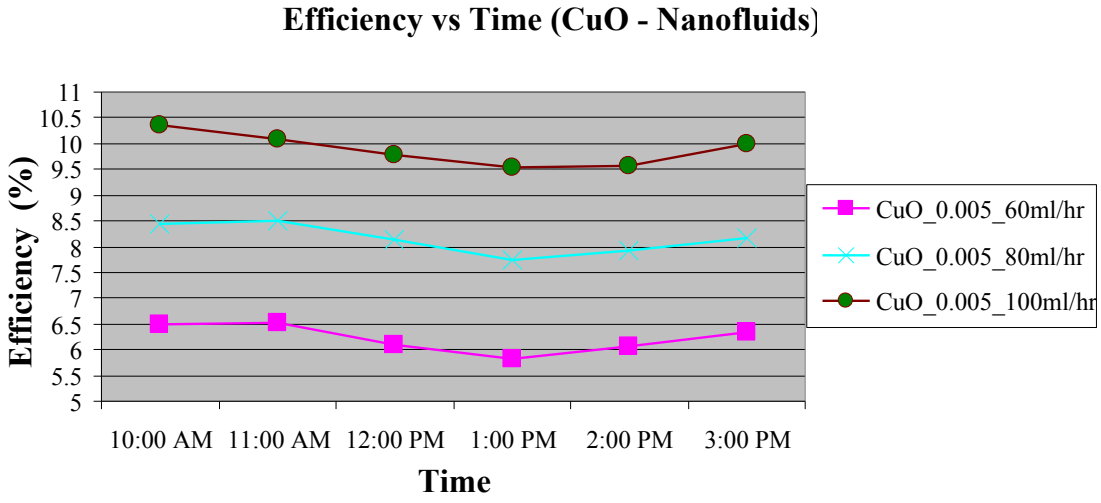

Fig. 5.7

Again Variation of temperature difference and collector efficiency shows the same profile for CuO nanofluid of volume fraction 0.005% through out the day. These variations are shown in Fig. 5.4 and 5.5. At mid day when solar irradiation is at its peak value efficiency has a lowest value and temperature difference has highest value. From the above plots it can be concluded that the efficiency of the collector is greater in case of CuO nanofluid (φ = 0.005%) then water as well as CuO nanofluid (φ = 0.005%).

1.1 Performance Comparison Charts of Solar Collector

1.1.1 Comparison charts between Water and CuO nanofluid (φ_P = 0.05%)

Temperature Difference Comparison:-

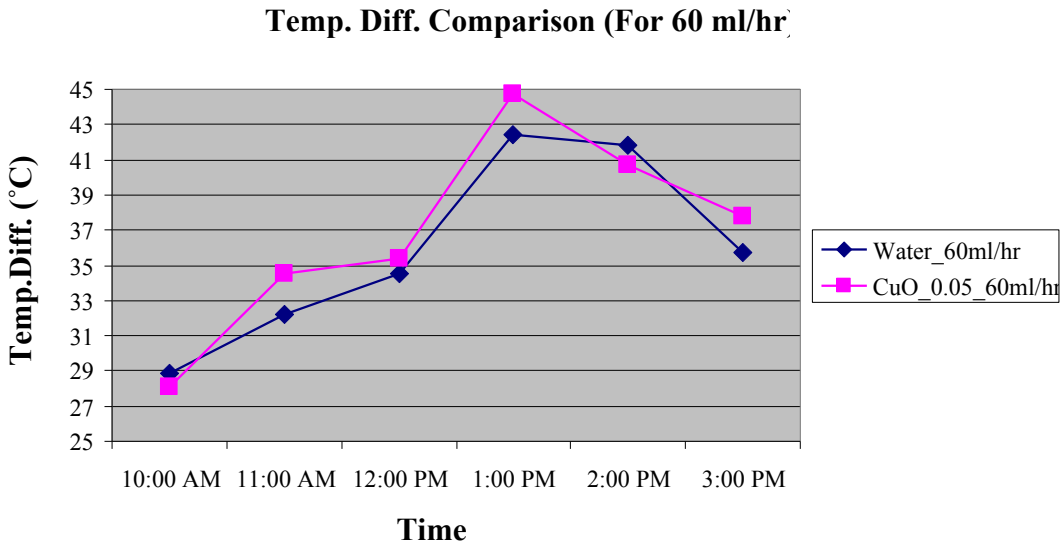

Fig. 5.8

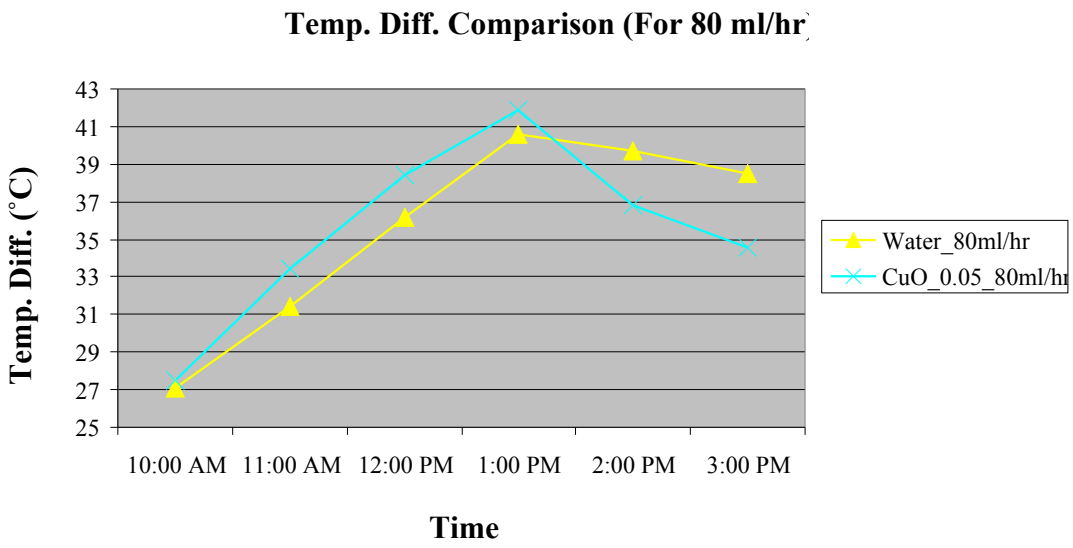

Fig. 5.9

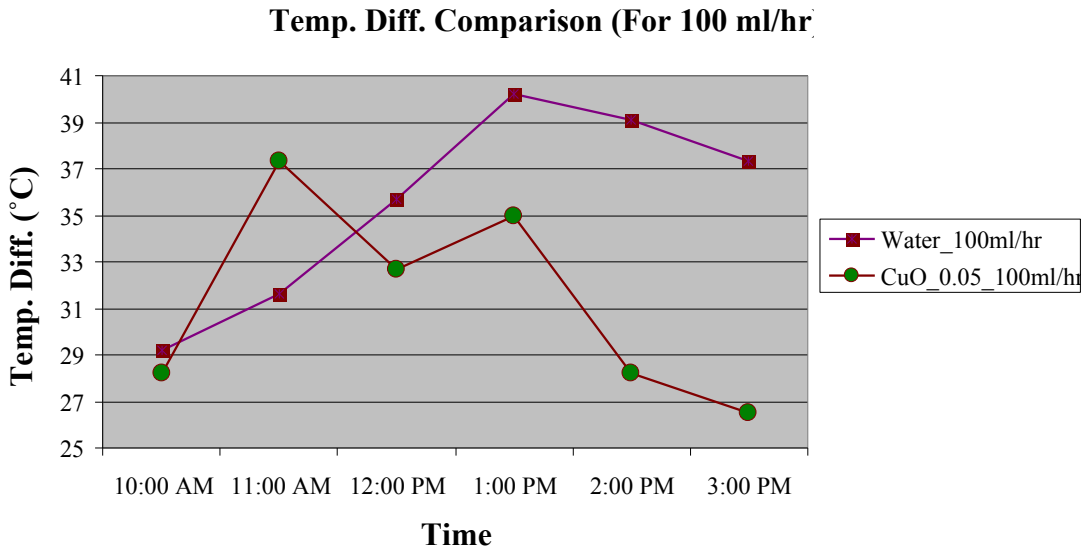

Fig. 5.10

Fig. 5.8, 5.9, 5.10 shows the variation of temperature difference, it can be seen from the plots that temperature difference is almost higher in case of CuO nanofluids then water. This variation is with in the range of 2˚C - 3˚C. One would expect these results since the thermal conductivity of CuO nanofluid is higher than water. In plot Fig. 5.10 CuO – nanofluid line going down it is so because at that day the radiation was not of good intensity.

Efficiency Comparison:-

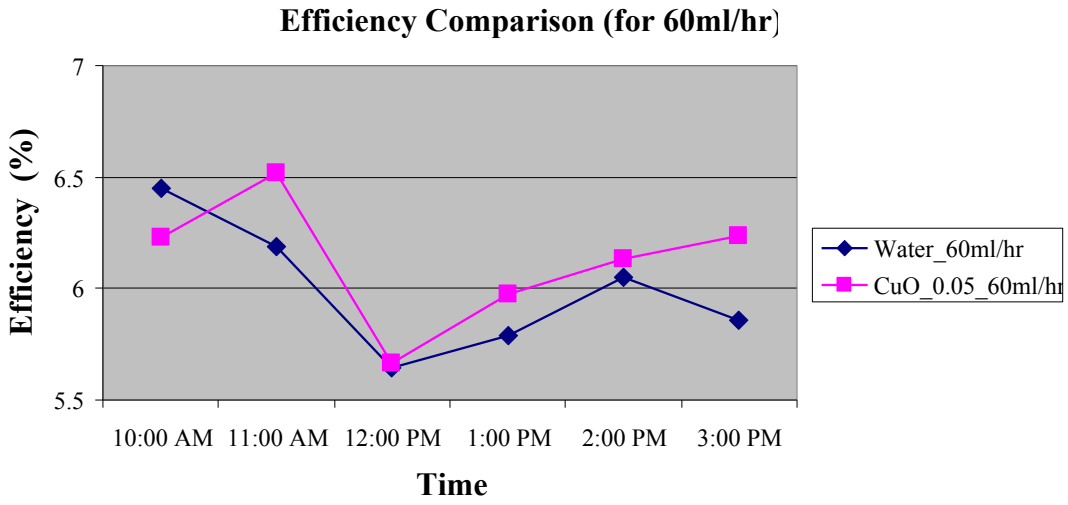

Fig. 5.11

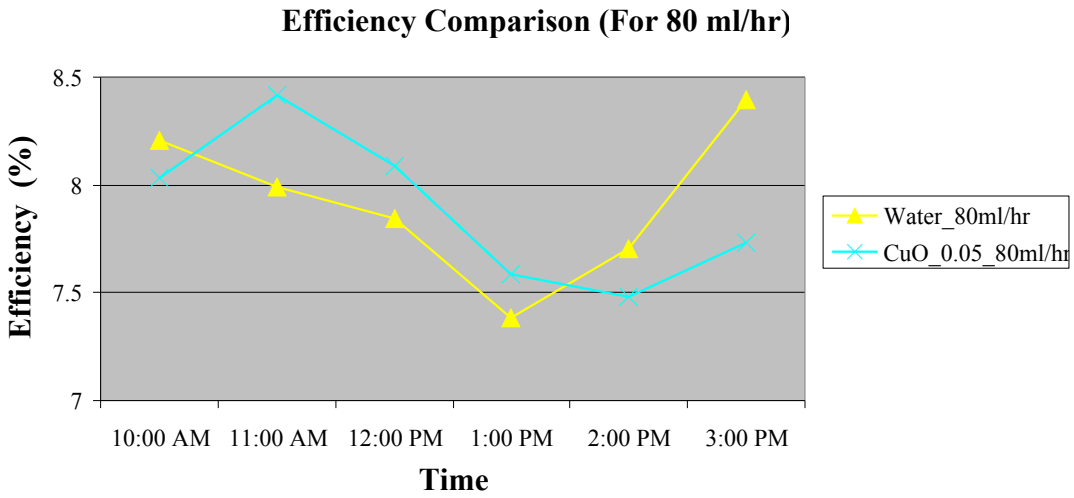

Fig. 5.12

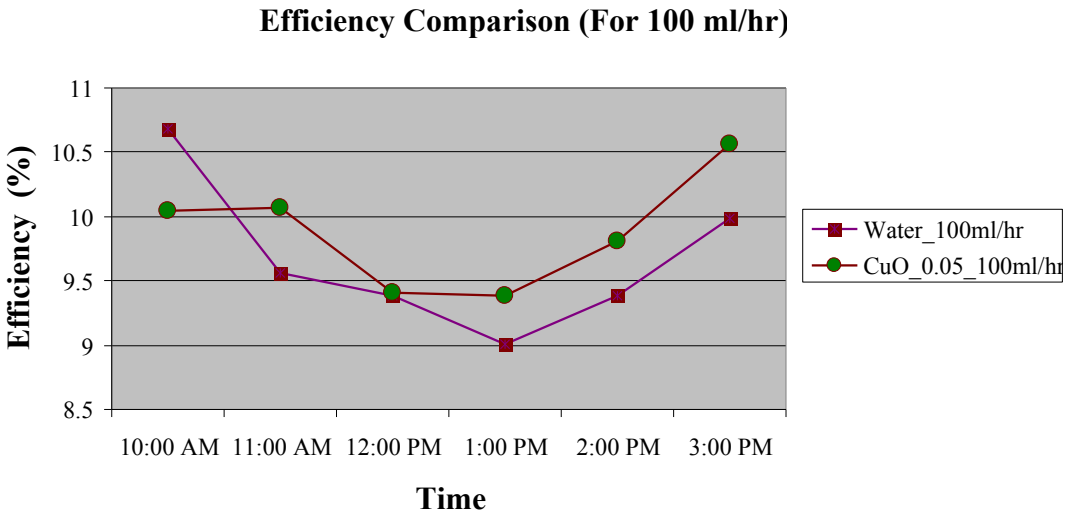

Fig. 5.13

Collector efficiency is a function of mass flow rate and temperature difference. As temperature difference of CuO nanofluid increases collector efficiency also increases for same mass flow rate. This might be because CuO nanofluid carries more heat then water. As mass flow rate increases collector efficiency increases for both water as well as CuO nanofluid. Also the surface area of CuO nanoparticle is higher due to extremely small size, which makes nanofluid based solar collector more efficient. These variations of efficiency are shown in Fig. 5.11, 5.12 and 5.13. When CuO nanoparticles are suspended in to water then due to the higher optical properties heat absorption capacity of nanofluid increases which give a higher temperature difference. The density of the CuO is higher then water, so after suspension the heat capacity of nanofluid increases, which in turn enhance the collector efficiency.

1.1.2 Comparison charts between Water and CuO nanofluid (φ_P = 0.005%)

Temperature Difference Comparison:-

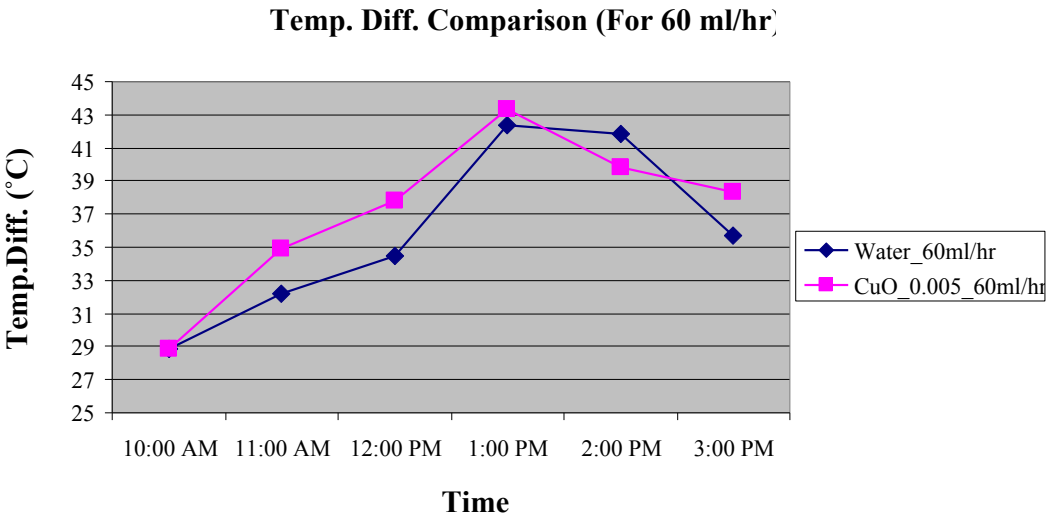

Fig. 5.14

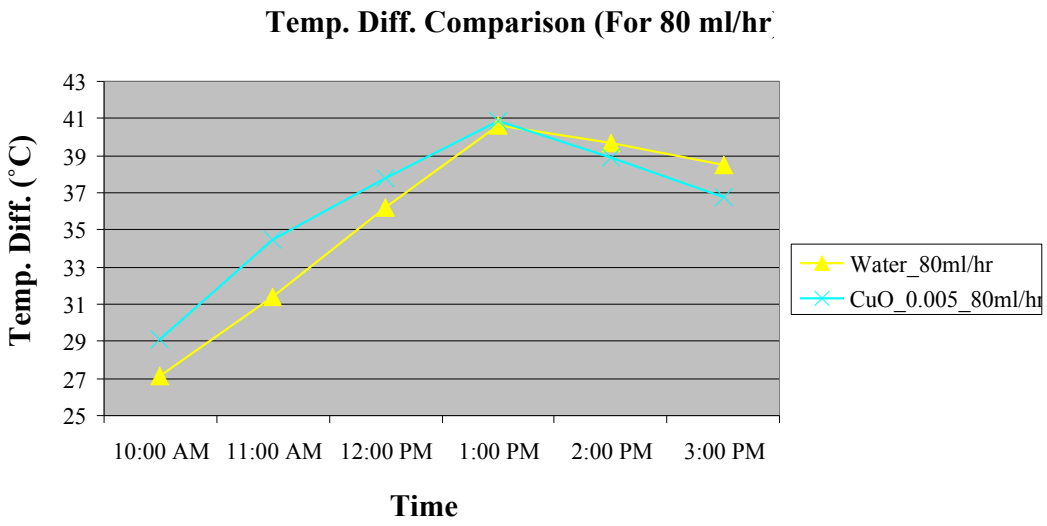

Fig. 5.15

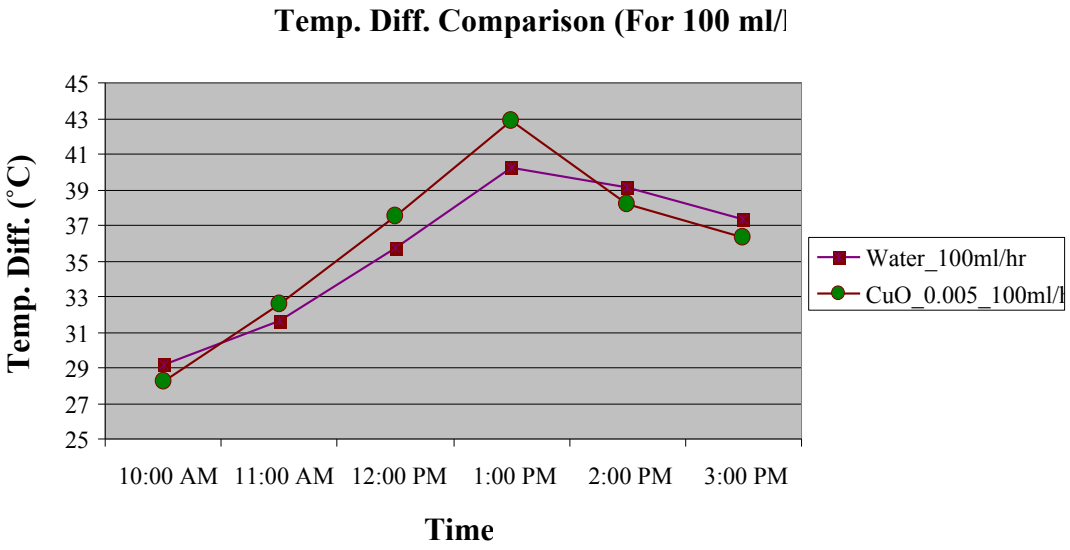

Fig. 5.16

In Fig. 5.14, 5.15, 5.16 the variation of temperature difference for lower volume fraction of CuO nanofluid. These plots show again an increase in variation of temperature difference with water but higher then the variation with the higher volume fraction. It might be possible because as volume fraction of CuO nanoparticles increases the heat absorption capacity also increases.

Efficiency Comparison:-

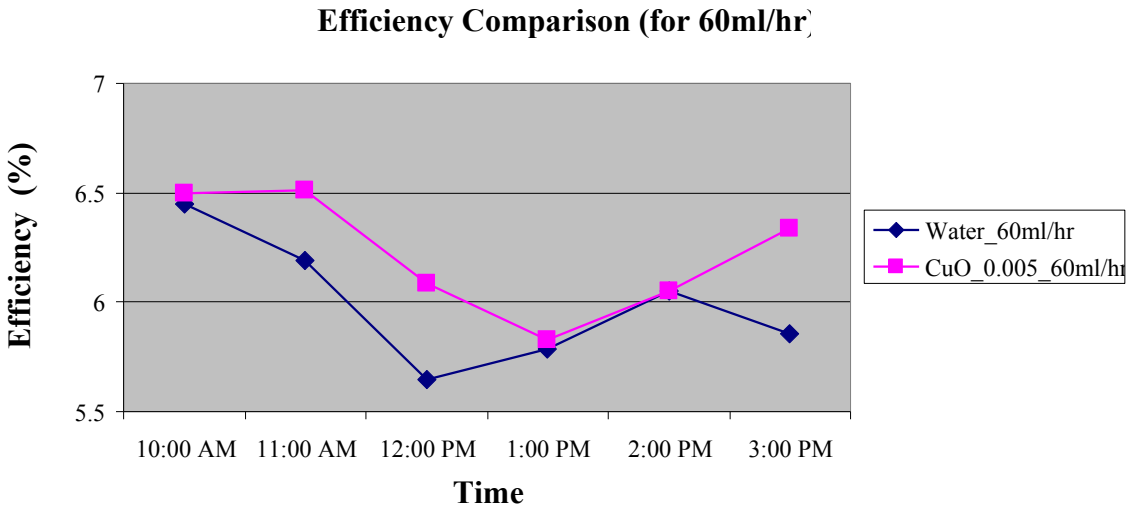

Fig. 5.17

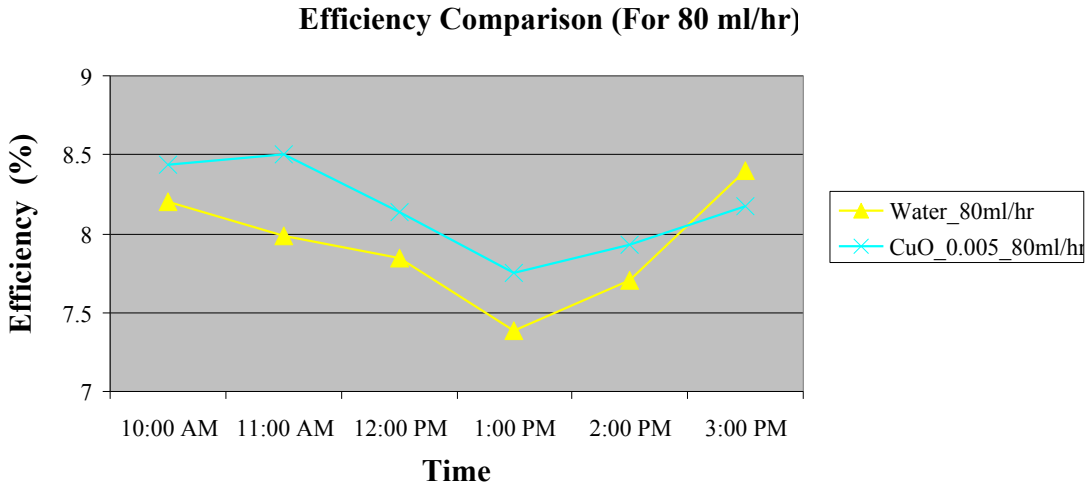

Fig. 5.18

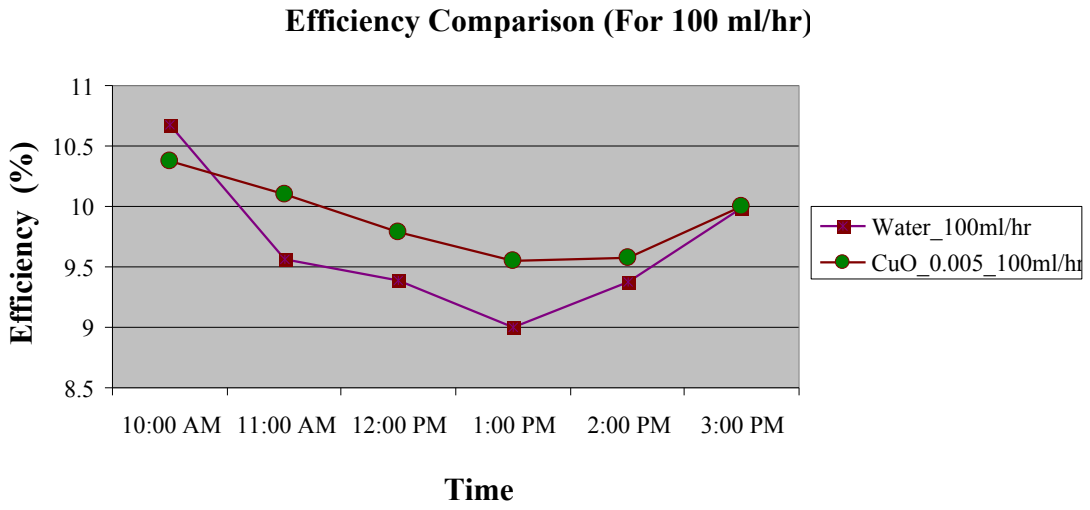

Fig. 5.19

An enhancement in collector efficiency can be seen in the above plots Fig. 5.17, 5.18, and 5.19. Thermal properties of nanofluids very much depend on size as well as volume fraction of nanoparticles in the base fluid. The heat transfer characteristics of nanofluids also depend on the sonication time of nanoparticles and the quality of sonication of nanofluid. So, as stated above CuO has higher value of thermal conductivity and thermo physical characteristics e.g. density, viscosity etc. which enhance the heat absorption capacity, the specific heat capacity and heat carrying properties of nanofluids.

1.1.3 Comparison charts between CuO nanofluid (φ_P = 0.05%) and CuO nanofluid (φ_P = 0.005%)

Temperature Difference Comparison:-

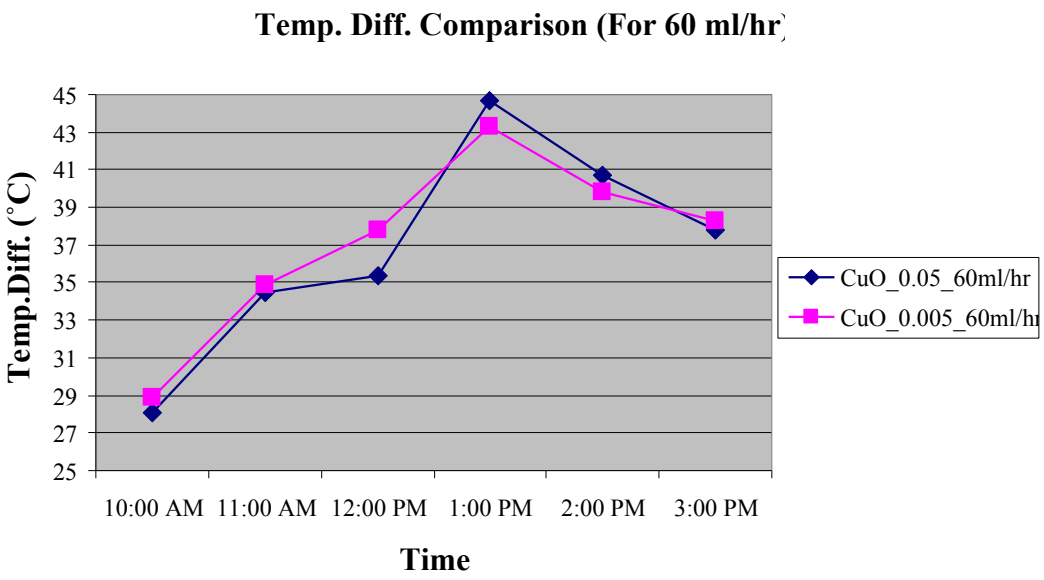

Fig. 5.20

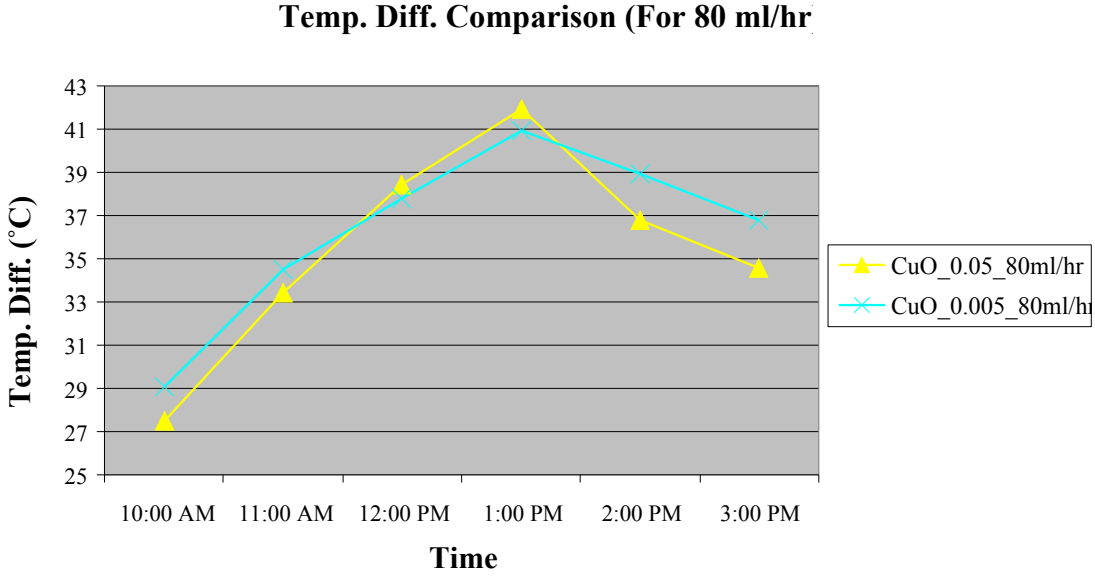

Fig.5.21

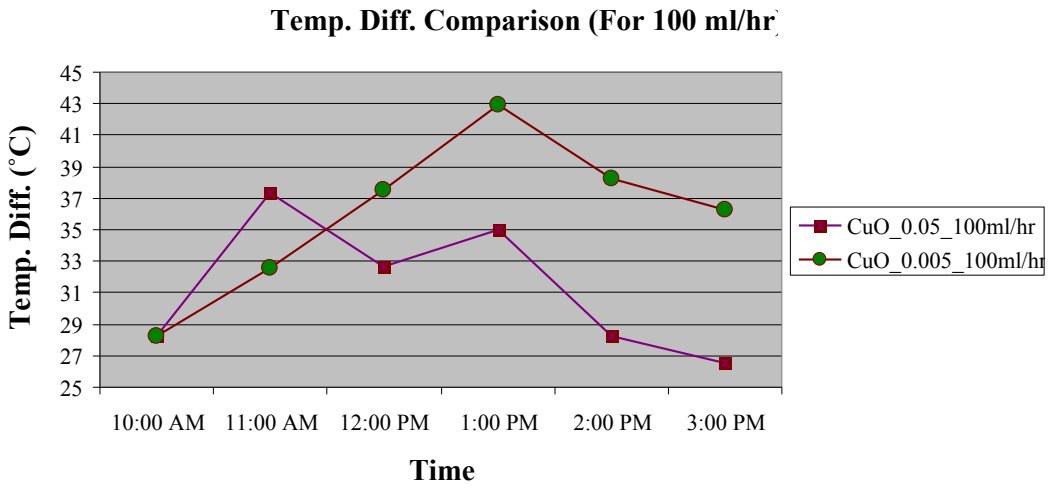

Fig. 5.22

By observing the plots Fig. 5.20, 5.21 and 5.22 it can be concluded that temperature difference of the nanofluid increases at lower volume fractions and so as efficiency of the collector, One possible reason for the lower performance at higher volume concentration is that nanofluids are unstable at high volume concentration that means the particles at high volume fraction agglomerate and become heavy and settle down which lower the absorption capacity of the nanofluid. Secondary reason might be that solar radiation gets absorbed in the upper layers of nanofluids of higher volume fraction because of high concentration.

Efficiency Comparison:-

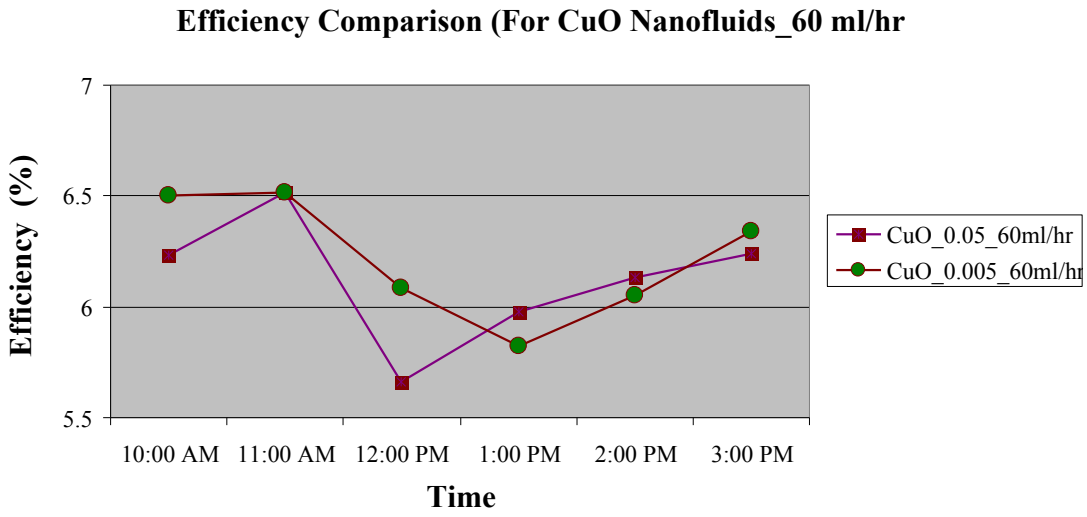

Fig. 5.23

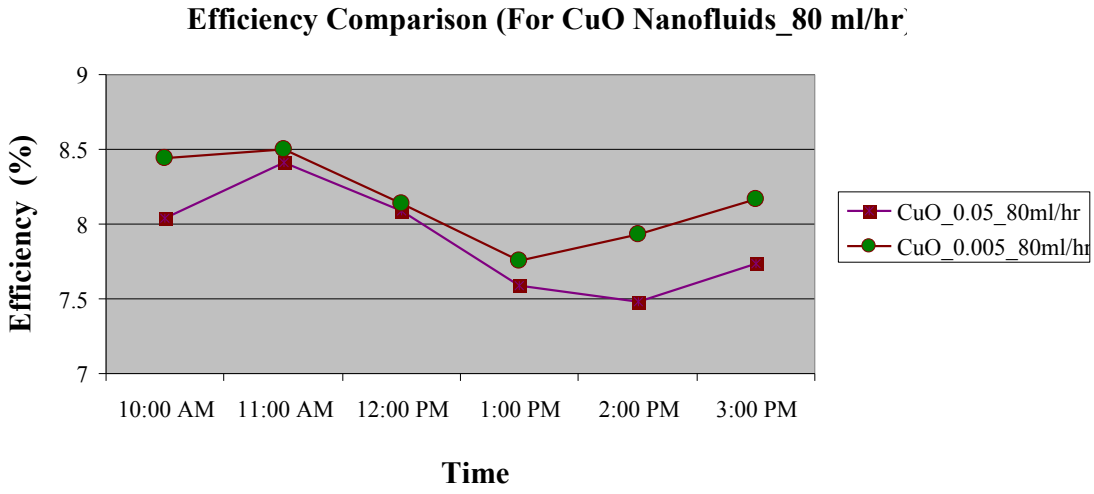

Fig. 5.24

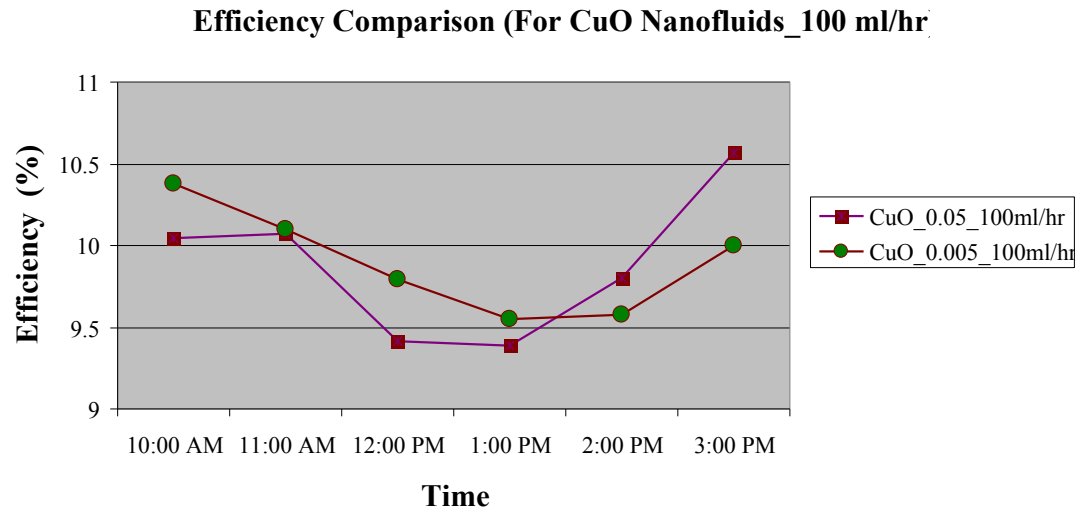

Fig. 5.25

It can be observed that same as the temperature difference collector efficiency of the nanofluid increases at lower volume fractions, the comparison graphs of variation of efficiency is shown in Fig. 5.23, 5.24 and 5.25. Thermo physical properties e.g density, viscosity, heat capacity etc. depend upon the volume fraction of nanoparticles in nanofluid, higher the volume concentration higher will be the density, viscosity as well as heat capacity. But here the collector efficiency decreases, so as stated above nanofluids confronts the problem of setteling down of nanoparticles as volume fraction of nanoparticle increases. So, for higher volume concentration sonication time will be more, so as nanoparticles settle down

nanofluid works as the conventional fluid

CHAPTER 6

CONCLUSION AND FUTURE SCOPE

The purpose of this thesis work is to perform an experiment and simplified analysis of how a nanofluid-based direct absorption solar thermal system (DASC) performance would compare to a conventional one. The concluded points of this work are as follows:

1. By using CuO nanofluids in DASC efficiency enhancement on the order of 4 – 6 %, when compared to water.
2. CuO nanofluid with 0.005% volume fraction posses 2 – 2.5 % of efficiency improvement than 0.05% volume fraction.
3. One of the main reasons of getting higher efficiency is the very small particle size, which enhances the absorption capacity of nanofluids so, improvement in efficiency could be obtained by using various particle size distribution.
4. There are also some demerits associated with nanofluids e.g. the settling of the nanoparticles in the base fluid, preparation and testing of nanoparticles are very much costly, which needs to be taken into consideration.
5. By overcoming the above problems the improvement of collector efficiency can be achieved up to 10 – 15 %.

Area of application of nanofluids in solar energy is a very new research field, there are also some contradictions in the results of some research work as it is the initial phase of implementing nanofluids in solar energy. So, there is a necessity of further theoretical as well as experimental work, investigations to enhance the efficiency of solar collector and to obtain firm and authenticate results. So, it can be concluded that nanofluids have a good potential in solar thermal application and nanofluid is the answer for the heat transfer limitation of conventional heat transfer fluids.

REFERENCES

[1] Minardi.J.E, Chuang.H.N, Solar Energy 17, 179 (1975)

[2] Das.K.S, Choi.S.U.S, YU.W, Pradeep.T, Nanofluids Science and Technology, ISBN 978-0-470-07473-2, Page (1-30)

[3] Otanicar.T.P, Phelan.P.E, Prasher.R.S, Rosengarton.G, Taylor.R.A, Nanofluid – Based direct absorption solar collector, (2010)

[4] Tyagi.H, Phelan.P, Prasher.R, Predicted Efficiency of a Low-Temerature Nanofluid based Direct Absorption Solar Collector, Journal of Solar Energy, Vol.131 (2009)

[5] Taylor.R.A, Phelan.P.E, Otanicar.T.P, Walker.C.A, Nguyen.M, Trimble.S, Prasher.R, Applicability of Nanofluids in high flux solar collectors, Journal of Renewable and Sustainable Energy 3,023104 (2011)

[6]Han.Z, Nanofluids with Enhanced Thermal Transport Properties, Department of Mechanical engineering, University of Maryland at collage park, (2008)

[7]Duffie.J.A, Beckman.W.A, Solar Engineering of Thermal Processes (Wiley, New York, (1988).

[8] U.S. Department of Energy - Energy Efficiency and Renewable Energy Solar Energy Technologies Program

[9] http://www.dg.history.vt.edu/ch2/conversion.html

[10] Pyranometer CMP -11 from Kipp & Zonen, http://users.du.se/~ffi/SERC/Hybrid/technical_data.htm

[11] Garg.H.P, Prakash.J, Soalr Energy Fundamental and Applications, Tata McGraw Hill, ISBN 0-07-463631-6, Page (35, 46,116), (1997).

[12] Sukhatme.S.P, Solar Energy (Principles of Thermal Collection and Storage), Tata Mcgraw Hill, ISBN 0-07-451946-8, (1984).

[13] Khanafer.K and Vafai.K, A Critical Synthesis of thermo physical characteristics of Nanofluids, International Journal of Heat and Mass Transfer (Under press), (2011)

[14] Zhou.K, Wang.R, Xu.B, Li.Y, Synthesis, Characterization and catalytic properties of CuO nano crystals with various shapes, Institute of Physics Publishing Ltd., Printed at UK, (2006)

[15] R.Winston, J.C.Minano, P.Benitez, Nonimaging Optics, Elsevier Academic Press, pp. 217, (2005)

[16] Rapp, Donald, Solar Energy, Prentice-Hall, Englewood Cliffs, NJ, (1981)

[17] Goswami, Yogi.D, Kreith, Frank, and Kreider, Jan F., Principles of Solar Engineering, 2nd edition. Taylor and Francis, Philadelphia, PA, (2000)

[18] Chang.M.H, Liu.H.S, Tai.C.Y, Preparation of Copper Oxide nanoparticles and its application in nanofluid, Powder Technology 207 (2011) 378 – 386.

[19] Newton.C.C, A Concentrated Solar Thermal Energy System, The Florida University, FAMU – FSU College of Engineering, (2007)

[20] Rai.G.D, Solar Energy Utilization, Khanna Publishers New Delhi, (1996)

[21] Kalogirou.S.A, Solar Thermal Collectors and Applications, Progress in Energy and Combustion Science, 30 (2004) 231 – 295.

[22] Yousefi.T, Veysi.F, Shojaeizadeh.E,Zinadini.S, An Experimental investigation on the effect of Al2O3 – H2O nanofluid on the efficiency of flat plate solar collectors, Renewable Energy 39 (2012) 293 – 298.

[23] Lenert.A, Nanofluid – based Receivers for High – Temperature, High – Flux Direct Solar Collectors, Massachusetts Institute of Technology (June 2010)

[24] Wang.X.Q, Mujumdar.A.S, Heat transfer characteristics of nanofluids: a review, International Journal of Thermal Sciences 46 (2007) 1 -19.

[25] Wang.X, Xu.X, Choi.S.U.S, Thermal conductivity of nanoparticle – fluid mixture, Journal of Thermo physics and Heat Transfer 13 (4) (1999) 474 – 480.

XRD details (sample purchased):

Measurement Conditions: (Bookmark 1)

Dataset Name	CuO BUYING
File name	C:\X'Pert Data\MAY2012\CuO BUYING.xrdml
Comment	Configuration=Flat Sample Stage, Owner=jagtar, Creation date=6/11/2007 3:57:00 PM
	Goniometer=PW3050/60 (Theta/Theta); Minimum step size 2Theta:0.001; Minimum step size Omega:0.001
	Sample stage=PW3071/xx Bracket
	Diffractometer system=XPERT-PRO
	Measurement program=PU, Owner=jagtar, Creation date=4/15/2008 1:52:59 PM
Measurement Date / Time	5/24/2012 4:59:25 PM
Operator	Panjab University
Raw Data Origin	XRD measurement (*.XRDML)
Scan Axis	Gonio
Start Position [°2Th.]	10.0084
End Position [°2Th.]	99.9894

Step Size [°2Th.]	0.0170
Scan Step Time [s]	25.1954
Scan Type	Continuous
PSD Mode	Scanning
PSD Length [°2Th.]	2.12
Offset [°2Th.]	0.0000
Divergence Slit Type	Fixed
Divergence Slit Size [°]	0.9570
Specimen Length [mm]	10.00
Measurement Temperature [°C]	25.00
Anode Material	Cu
K-Alpha1 [Å]	1.54060
K-Alpha2 [Å]	1.54443
K-Beta [Å]	1.39225
K-A2 / K-A1 Ratio	0.50000
Generator Settings	40 mA, 45 kV
Diffractometer Type	0000000011023505
Diffractometer Number	0
Goniometer Radius [mm]	240.00
Dist. Focus-Diverg. Slit [mm]	91.00
Incident Beam Monochromator	No
Spinning	No

Main Graphics, Analyze View: (Bookmark 2)

Peak List: (Bookmark 3)

Pos. [°2Th.]	FWHM [°2Th.]	d-spacing [Å]	Rel. Int. [%]	Area [cts*°2Th.]
32.5915	0.2676	2.74751	8.07	35.59
35.5914	0.3680	2.52250	100.00	606.43
38.7931	0.3011	2.32137	85.70	425.20
48.9210	0.2175	1.86187	19.06	68.30
53.5925	0.4684	1.71008	5.25	40.49
58.3667	0.4015	1.58107	8.51	56.33
61.5598	0.2844	1.50650	13.28	62.21
66.5732	0.4684	1.40470	8.88	68.50
68.1152	0.2676	1.37661	11.51	50.76
72.4928	0.4684	1.30389	4.36	33.68
75.3083	0.5712	1.26094	6.37	81.09

XRD detailed (sample prepared at laboratory):

Measurement Conditions: (Bookmark 1)

Dataset Name CuO-PRASHANT

File name	C:\X'Pert Data\MAY2012\CuO-PRASHANT.xrdml
Comment	Configuration=Flat Sample Stage, Owner=jagtar, Creation date=6/11/2007 3:57:00 PM
	Goniometer=PW3050/60 (Theta/Theta); Minimum step size 2Theta:0.001; Minimum step size Omega:0.001
	Sample stage=PW3071/xx Bracket
	Diffractometer system=XPERT-PRO
	Measurement program=PU, Owner=jagtar, Creation date=4/15/2008 1:52:59 PM
Measurement Date / Time	5/28/2012 9:47:32 AM
Operator	Panjab University
Raw Data Origin	XRD measurement (*.XRDML)
Scan Axis	Gonio
Start Position [°2Th.]	10.0084
End Position [°2Th.]	99.9894
Step Size [°2Th.]	0.0170
Scan Step Time [s]	25.1954
Scan Type	Continuous
PSD Mode	Scanning
PSD Length [°2Th.]	2.12
Offset [°2Th.]	0.0000
Divergence Slit Type	Fixed
Divergence Slit Size [°]	0.9570
Specimen Length [mm]	10.00

Measurement Temperature [°C]	25.00
Anode Material	Cu
K-Alpha1 [Å]	1.54060
K-Alpha2 [Å]	1.54443
K-Beta [Å]	1.39225
K-A2 / K-A1 Ratio	0.50000
Generator Settings	40 mA, 45 kV
Diffractometer Type	0000000011023505
Diffractometer Number	0
Goniometer Radius [mm]	240.00
Dist. Focus-Diverg. Slit [mm]	91.00
Incident Beam Monochromator	No
Spinning	No

Main Graphics, Analyze View: (Bookmark 2)

Peak List: (Bookmark 3)

Pos. [°2Th.]	FWHM [°2Th.]	d-spacing [Å]	Rel. Int. [%]	Area [cts*°2Th.]
29.7590	0.1338	3.00224	9.52	16.59
32.8826	0.3011	2.72385	7.21	28.27
35.8262	0.2509	2.50651	100.00	326.81

39.0960	0.3346	2.30408	86.41	376.54
49.0335	0.2175	1.85786	18.67	52.89
58.6147	0.4015	1.57497	8.10	42.37
61.9581	0.3346	1.49777	13.62	59.36
66.5499	0.4896	1.40397	11.20	96.52